Journal of Visualized Experiments

Evaluation of stem cell therapies in a bilateral patellar tendon injury model in rats

--Manuscript Draft--

Article Type:	Invited Methods Article - JoVE Produced Video
Manuscript Number:	JoVE56810R2
Full Title:	Evaluation of stem cell therapies in a bilateral patellar tendon injury model in rats
Keywords:	Rat model; Tendon injury model; mesenchymal stem cells; Chitosan; spheroids
Corresponding Author:	Dominique Griffon Western University of Health Sciences Pomona, CA UNITED STATES
Corresponding Author's Institution:	Western University of Health Sciences
Corresponding Author E-Mail:	dgriffon@westernu.edu
First Author:	John Wagner
Other Authors:	John Wagner
	Takashi Taguchi
	Jane Cho
	Chandrashekhar Charavaryamath
Author Comments:	
Additional Information:	
Question	**Response**
If this article needs to be "in-press" by a certain date, please indicate the date below and explain in your cover letter.	

TITLE:
Evaluation of Stem Cell Therapies in a Bilateral Patellar Tendon Injury Model in Rats

AUTHORS AND AFFILIATIONS:
John R Wagner[1], Takashi Taguchi[1], Jane Y Cho[2], Chandrashekhar Charavaryamath[3], Dominique J Griffon[1]

[1]College of Veterinary Medicine
Western University of Health Sciences
Pomona, United States of America

[2]Applied Medical
Rancho Santa Margarita, United States of America

[3]College of Veterinary Medicine
Iowa State University
Ames, United States of America

EMAIL ADDRESSES:
John R Wagner (jrwagner@westernu.edu)
Takashi Taguchi (taguchit@westernu.edu)
Jane Y Cho (chyoungmi@gmail.com)
Chandrashekhar Charavaryamath (chandru@iastate.edu)
Dominique J Griffon (dgriffon@westernu.edu)

CORRESPONDING AUTHOR:
Dominique J Griffon (dgriffon@westernu.edu)
College of Veterinary Medicine,
Western University of Health Sciences
Pomona, U.S.

KEYWORDS:
Rat model, Tendon injury model, Mesenchymal stem cells, Chitosan, Spheroids, Patellar tendon window defect

SHORT ABSTRACT:
This paper describes the preparation and evaluation of umbilical cord matrix-derived mesenchymal stem cells spheroids with a bilateral patellar tendon defect model in a rat. This model was associated with an acceptable morbidity and was found to detect differences between untreated and treated tendons, and between the two treatments tested.

LONG ABSTRACT:
Regenerative medicine provides novel alternatives to conditions that challenge traditional treatments. The prevalence and morbidity of tendinopathy across species, combined with the

limited healing properties of this tissue, have prompted the search for cellular therapies and propelled the development of experimental models to study their efficacy. Umbilical cord matrix-derived mesenchymal stem cells (UCM-MSC) are appealing candidates because they are abundant, easy to collect, circumvent the ethical concerns and risk of teratoma formation, yet resemble primitive embryonic stem cells more closely than adult tissue-derived MSCs. Significant interest has focused on chitosan as a strategy to enhance the properties of MSCs through spheroid formation. This paper details techniques to isolate UCM-MSCs, prepare spheroids on chitosan film, and analyze the effect of spheroid formation on surface marker expression. Consequently, creation of a bilateral patellar tendon injury model in rats is described for *in vivo* implantation of UCM-MSC spheroids formed on chitosan film. No complication was observed in the study with respect to morbidity, stress rising effects, or tissue infection. The total functional score of the operated rats at 7 days was lower than that of normal rats, but returned to normal within 28 days after surgery. Histological scores of tissue-healing confirmed the presence of a clot in treated defects evaluated at 7 days, absence of foreign body reaction, and progressing healing at 28 days. This bilateral patella tendon defect model controls inter-individual variation via creation of an internal control in each rat, was associated with acceptable morbidity, and allowed detection of differences between untreated tendons and treatments.

INTRODUCTION:

Tendon injury is one of the most common causes of significant pain and muscle atrophy across species[1]. In veterinary medicine, tendon and ligament injuries are of special interest in horses, as 82% of all injuries in race horses involve the musculoskeletal system, and 46% of those affect tendons and ligaments[2,3]. Scar tissue formation affects the biomechanical properties of healed tendons and explains the guarded prognosis for return to athletic use after flexor tendon injuries; re-injury occurs within 2 years in up to 67% of horses treated conservatively[4]. Regenerative medicine provides novel alternatives to a condition that challenges traditional treatments. Autologous stem cell therapy has produced some encouraging results[5,6] but is limited by the morbidity associated with tissue collection, delayed administration due to processing/reprogramming of cells, and the influence of the patient's health status (such as age) on the properties of stem cells[7,8]. These limitations provide a rationale for investigating allogeneic stem cells as an off-the-shelf alternative. Fetal adnexa-derived cells are appealing candidates because they circumvent the ethical concerns and risk of teratoma formation associated with embryonic stem cells. Among fetal adnexa, umbilical cord matrix (UCM), also named Wharton's Jelly, is abundant and easy to collect.

Regardless of cell source, enhancing stemness is essential to establish a cell bank for allogenic regenerative medicine. From a functional standpoint, stemness can be defined as the potential for self-renewal and multi-lineage differentiation[9]. Evidence of stemness relies on proliferation and differentiation assays, along with expression of gene markers *Oct4*, *Sox2,* and *Nanog*[9]. One strategy to enhance stemness relies on the use of biomaterials to serve as void fillers and carriers enhancing proliferation and differentiation of UCM-MSCs. This approach eliminates concerns regarding manipulation of transcriptional factors to reprogram mature cells into induced pluripotent cells. Among biomaterials considered as potential carriers for stem cells, chitosan is appealing for its biocompatibility and degradability[10]. This natural aminopolysaccharide is formed

by alkaline deacetylation of chitin, the second most abundant natural polysaccharide, primarily obtained as a subproduct of shellfish[10]. We have previously investigated interactions between MSCs and chitosan scaffolds, and observed the formation of spheroids[11-16]. We also reported on the superiority of chondrogenesis on chitosan matrices[12,13,15-18]. More recently, two independent studies described spheroids formation by adipose tissue and placenta tissue derived MSCs cultured on a chitosan film[19,20]. This formation of spheroids not only enhanced stemness, but also improved the retention of stem cells after *in vivo* implantation[20].

The prevalence and morbidity of tendinopathy across species have prompted the development of experimental models to study the pathophysiology of tendinopathies and test new therapies such as stem cell injections. In horses, collagenase-induced tendonitis is a common model to demonstrate efficacy using MSCs in tendon repair[21]. The relevance of this approach is limited, as injections cause acute inflammatory changes, whereas clinical tendinopathies usually result from chronic overstrain[22,23]. In addition, chemical induction of tendon disease induces a healing response and does not replicate the impaired healing process present in clinical cases[22,23]. Excision of a segment of the superficial digital flexor tendon has been described as a surgical model of tendonitis in horses[24]. More recently, a minimally invasive approach was used to restrict the traumatic damage to the central core of the superficial digital flexor tendon[25]. Surgical models do not simulate the fatigue mechanism that may lead to natural tendon disease, and tend to lack reproducibility in the extent of damage created[25]. Regardless of the model, the morbidity and cost associated with equine models of tendon diseases are additional limitations, which justify an interest in rodent models as a first step for *in vivo* evaluation of novel therapies.

One of the main advantages of experimental models in rodents consists of the cost and ability to control inter-individual variability. Rodents can be standardized with respect to various physiological factors due to their rapid growth rates and relatively short life spans, limiting sources of variation and therefore reducing the number of animals required to detect differences. Strategies to induce tendon diseases in rodents have relied on chemical induction, but also on surgical creation of partial tendon defects[21]. Surgical models may simulate natural tendinopathies better than chemical models, but can lead to higher morbidity and catastrophic failure of the damaged tendon. In that respect, rats seem better candidates than mice for these models, as their size allows creation of larger defects, thereby facilitating evaluation of tissue healing. Sprague-Dawley rats have been used in experimental studies of tendinopathies in four major tendon groups: rotator cuff, flexor, Achilles, and patellar tendons[26]. Among these, models involving the patellar tendon are especially appealing because of the larger size of this tendon and the ease of accessing it[27]. The patellar tendon attaches the quadriceps muscle to the tibial tuberosity. Within this extensor mechanism, the patella is a sesamoid bone that directs the action of the quadriceps and delineates the proximal extent of the patellar tendon. The presence of bony anchors at the proximal and distal extents of the patellar tendon facilitates biomechanical tests. Models involving the patellar tendon typically rely on unilateral surgical defects, with a contralateral intact tendon serving as a control[28,29]. The most common patellar tendon defect model involves excising the central portion (1 mm in width) of the patellar tendon from the distal apex of the patella to the insertion of the tibial tuberosity, while the contralateral patellar tendon is left intact. Measures of outcomes have included histology, non-destructive biomechanical

testing or biomechanical testing to failure, ultrasound imaging, *ex vivo* fluorescence imaging, gross observation, and functional tests[28,30,31]. Unilateral models do not allow comparison of a proposed treatment with conservative management of a similar injury within the same animal. Similarly, comparison between several treatments requires separate animals. A bilateral model would eliminate inter-individual variations and reduce the number of animals required for a study[32]. However, bilateral injuries may increase morbidity, and bilateral lameness could impede treatment evaluation. A few studies briefly report the use of bilateral patellar tendon defects in rats but focus on the effects of treatments rather than peri-operative management and morbidity of the model[33,34].

This study's long-term goal is to develop a strategy to improve stemness and *in vivo* survival of UCM-MSCs destined to allogenic transplantation. To achieve this goal, we have recently reported improved stemness of UCM-MSCs by formation of spheroids on chitosan film and incubation under hypoxic environment[35]. These *in vitro* properties were associated with improved biomechanical properties of patellar tendon defects treated with conditioned UCM-MSCs. Based on these results, the rat bilateral patellar tendon defect model seems suitable to test candidate treatments for tendon injuries[36]. The purpose of the study reported here is to provide detailed protocols for isolation and characterization of UCM-MSCs, preparation of a biologic delivery system for stem cells, creation and treatment of bilateral patella tendon defects, and post-operative recovery and evaluation of tissue healing within the defects.

PROTOCOL:

All methods described here have been approved by the Institutional Animal Care and Use Committee (IACUC) of Western University of Health Sciences.

1. Isolation and Expansion of MSCs from Equine Umbilical Cord Matrix

1.1. Obtain the placenta from an adult mare (pregnant) after observed foaling and aseptically isolate the umbilical cord from the placenta. Keep the umbilical cord in phosphate buffered saline (PBS) with 1% penicillin-streptomycin (P/S) at 4 °C during transfer until processing.

1.2. Wash the umbilical cord twice with room temperature PBS with 1% P/S in a 50-mL tube. Section the umbilical cord into 2-inch-long fragments on 150-mm plate and wash in room temperature PBS with 1% P/S in a 50 mL tube two or three times, until most of the blood is rinsed out.

1.3. Cut the umbilical cord longitudinally to expose vessels. Remove vessels, including 2 arteries, a vein, and an allantoic stalk from the cord using forceps and scissors. Collect umbilical cord matrix (Wharton's Jelly), which is the jelly-like matrix surrounding vessels, onto a 150-mm plate by scraping with a scalpel, and mince the jelly into fine pieces.

1.4. Place Wharton's Jelly from 2-3 umbilical cord fragments (approximately 12-15 g) in a 50-mL tube with 15 mL of 0.1% (w/v) collagenase type IA solution in PBS. Incubate at 37 °C with gentle shaking for 3-4 h until dissolved.

1.5. Centrifuge digested tissue at 300 x g for 15 min and aspirate supernatant. Resuspend digested tissue in 15 mL of room temperature PBS with 1% P/S, mix by pipetting, centrifuge at 150 x g for 5 min, and aspirate supernatant (wash). Repeat washing twice more.

1.6. Resuspend washed cells in 15 mL of room temperature PBS with 1% P/S, mix by pipetting, strain by with 100-µm cell strainer, centrifuge at 150 x g for 5 min, and aspirate supernatant.

1.7. Prepare culture medium (CM) by mixing low glucose Dulbecco's Modified Eagle's Medium (LG-DMEM) with fetal bovine serum (FBS) and 1% P/S. Sterilize the medium by filtration.

1.8. Resuspend strained cells in 10 mL of CM pre-warmed to 37 °C, mix by pipetting, transfer into a 25 cm^2 tissue culture flask, and incubate in 5% CO_2 at 90% humidity and 37.0 °C. Change CM every 3 days until the culture reaches 70-80% confluence, when the culture will be passaged.

1.9. To passage the culture, aspirate CM from flask, wash with 5 mL of room temperature PBS twice, and detach with 3 mL of 0.25% trypsin/ethylenediaminetetraacetic acid (EDTA) at 37 °C for 5 min.

1.10. Neutralize trypsin/EDTA with 6 mL of CM pre-warmed to 37.0 °C, mix by pipetting, transfer into a 15-mL tube, centrifuge at 150 x g for 5 min, and aspirate supernatant. Resuspend detached cells in 1 mL of CM, mix by pipetting. Count the viable cells using trypan blue and hemocytometer. Re-seed into a 25 cm^2 tissue culture flask at 5,000 cells/cm^2, and incubate in 5% CO_2 at 90% humidity and 37.0 °C.

2. Preparation of Spheroids with UCM-MSCs Cultured on Chitosan Films

2.1. To prepare 100 mL of 1% (w/v) chitosan solution, add 1 g of chitosan in 99 mL of distilled water (dH_2O), and mix well with a magnetic stirrer.

2.2. Add 670 µL of glacial acetic acid and continue mixing until chitosan dissolves and becomes viscous. This usually takes 3-4 h.

2.3. Add 500 µL of chitosan solution into each well of the 12-well tissue culture plate, and swirl the plate to distribute chitosan solution evenly and cover all of the bottom surface.

2.4. Dry the chitosan solution coated plate under laminar flow cabinet without a cover overnight for 24 h. Once dried, thin film will be formed and adhered to plate.

2.5. Neutralize chitosan film by adding 1 mL of 0.5 N sodium hydroxide (NaOH) solution into each well and incubate for 2 h at room temperature. Aspirate NaOH from each well and wash each well with 1 mL of dH_2O three times. Wash each well with 1 mL of 70% ethanol (EtOH) once.

2.6. To sterilize chitosan film, add 1 mL of 70% EtOH into each well and incubate overnight in

laminar flow cabinet. Aspirate remaining EtOH from each well in the following day. Wash each well with 1 mL of sterile PBS three times. Sterilize chitosan film with ultraviolet light under laminar flow cabinet overnight without a cover.

2.7. To form spheroids of UCM-MSCs, seed expanded and passaged cells into each well at 5,000 cells/cm^2, and incubate in 5% CO_2 at 90% humidity and 37.0 °C.

Note: Cells can be incubated under hypoxia or normoxia, depending on the investigator's interest.

3. Expression of Surface Markers Analyzed via Flow Cytometry

3.1. Preparation of a single cell suspension

3.1.1. Standard plate

3.1.1.1. Remove medium from each well and wash twice with room temperature PBS.

3.1.1.2. Detach cells with 500 µL of a cell dissociation reagent into each well of a 12-well plate for 5-10 min at room temperature.

3.1.1.3. After incubation, add 1 ml of staining buffer (PBS containing 0.5% BSA) into each well and mix by pipetting to detach cells.

3.1.1.4. Transfer cell suspension into 15 mL conical tube and centrifuge at 150 x g for 5 min.

3.1.2. Chitosan plate

3.1.2.1. Collect all spheroids by aspirating medium using a pipette with a 1,000 µL tip. Transfer collected medium into a 15-mL conical tube. After collecting medium, wash well by adding 1 mL of PBS, and transfer washed PBS into the same 15 mL conical tube.

3.1.2.2. Centrifuge spheroids at 150 x g for 5 min and remove supernatant.

3.1.2.3. Add 500 µL of the cell dissociation reagent (*e.g.*, accutase) and incubate for 5-10 min at room temperature. Mix by pipetting using a 1 mL tip until spheroids dissociate and are no longer visible.

3.1.2.4. Add 1 mL of staining buffer into the single cell suspension and centrifuge at 150 x g for 5 min.

3.2. Washing cells

3.2.1. Remove the supernatant from the conical tube and re-suspend the cells in 3 mL of cold staining buffer. Keep cells on ice throughout experiment from this step.

3.2.2. Centrifuge at 300 x g for 5 min (washing).

3.2.3. Wash twice.

3.3. **Staining cells**

3.3.1. Centrifuge at 300 x g for 5 min and remove supernatant.

3.3.2. Count viable cells using a trypan blue and hemocytometer. Re-suspend 1 x 10^6 cells in 50 µL blocking buffer (PBS containing 10% horse serum) and incubate for 30 min on ice.

3.3.3. Add 10 µL fluorescein isothiocyanate (FITC) conjugated antibodies (CD44, CD90, CD105, CD34, major histocompatibility complex (MHC) class II, or isotype control for each antibody) and 40 µL of staining buffer, then incubate protected from light for 1 h on ice.

3.3.4. Add 3 mL of cold staining buffer and mix, centrifuge at 300 x g for 5 min, and aspirate supernatant (washing).

3.3.5. Repeat washing twice.

3.3.6. Re-suspend the cell pellet in 0.5 mL of staining buffer

3.3.7. Add 5 µL of 7-AAD (viability dye) and incubate for 30 min on ice

3.3.8. Analyze stained cell samples by flow cytometer. Exclude debris by their smaller SSC and FSC, and identify viable cells with lower uptake of 7-AAD. Plot FL1 and FL2 on the y- and x- axes, respectively. Use isotype control to create a gate above the diagonal line. Measure the percentage of positively stained cells in the area. Count at least 20,000 events/sample (**Supplementary Figure 1**).

3.3.9. Measure the percentage of cells stained with antibodies by gating viable cells and auto-fluorescence, and subtract percentage of cells stained with isotype control.

4. Bilateral Patellar Tendon Defect Model in Rat

4.1. Select Sprague-Dawley rats (adult male, 4-5 months old, body weight 350-375 g). Note the relatively large size of the rats used for this model.

4.2. Anesthetize the rat with 8% sevoflurane in 2 L/min 100% oxygen delivered via mask, until disappearance of pinch-toe reflex in the induction chamber.

4.3. Administer an intramuscular injection of Meloxicam (1 mg/kg) as preemptive analgesia.

4.4. Place the rat between two 0.5 L water bottles filled with warm water and covered with a cloth to maintain body temperature and position, while preventing skin injury. Tape each extremity to the table with tape. To reduce risk of hypothermia, cover the body with bubble wrap (**Figure 1**).

4.5. Maintain anesthesia with continuous flow of 5% sevoflurane in 1 L 100% oxygen mixture via nose cone, with the animal on dorsal recumbency on water heating pad.

4.6. To avoid skin trauma, do not clip the surgical sites. Instead, apply hair remover cream over both stifles. Use a tongue depressor to remove the cream and hair.

4.7. Scrub the surgical site with chlorhexidine digluconate scrub, and rinse with 70% ethanol 3 times.

4.8. Incise the skin with a #15 scalpel blade in a proximal to distal direction, on the craniomedial aspect of the stifle. Start the incision about 1 cm proximal to the level of the patella, and extend it approximately 5 mm distal to the tibial tubercle.

4.9. Reflect the skin to expose the patellar tendon by freeing the underlying subcutaneous tissue with a #15 scalpel blade.

4.10. Using the #15 scalpel blade, excise the central third of each patellar tendon (1 mm) from the distal aspect of the patella to the tibial tuberosity.

4.10.1. Align a 0.99 mm-diameter Kirschner wire against the tendon as a template to standardize the size of the defect in each limb (**Figure 2**).

4.10.2. Make 2 full-thickness incisions on each side of the Kirschner wire with a #15 scalpel blade to isolate the central portion of the tendon (**Figure 3**). Resect the central section proximally and distally with fine Iris scissors (**Figure 4**).

4.10.3. Before closing the fascia of the stifle, insert the clot (mixed cell suspension and ACP) for the appropriate treatment groups as described in 5.5. Close the fascia with a cruciate pattern and skin with an intradermal pattern using 5-0 polyglactin 910 sutures (**Figure 5**).

4.11. Repeat the procedure on the contralateral stifle.

Note: One defect is randomly assigned to a treatment (stem cells conditioned on chitosan or cultured on standard plates). The contralateral defect is left empty, to serve as internal control.

4.12. After surgery, administer 4 tablets of enrofloxacin (2 mg/tablet, orally, once daily) and a

tablet of meloxicam (2 mg/tablet, orally, once daily) for 7 days.

5. Delivery of MSCs within the Patellar Tendon Defect

5.1. Anesthetize a healthy rat which is not used for patellar tendon defect creation with 8% sevoflurane in 2 L/min 100 % oxygen delivered via mask, until disappearance of pinch-toe reflex in the induction chamber.

5.2. Collect 5 mL blood by cardiac puncture from the anesthetized Sprague-Dawley rat (adult male, 4-5 months old, body weight 350-375 g), in a 5-mL syringe with a 20-gauge needle containing 1 mL of acid-citrate-dextrose (5:1 v/v).

5.3. Euthanize the rat after cardiac puncture and blood collection, by intracardial injection of pentobarbital (100 mg/kg), while under the same anesthesia.

5.4. Centrifuge the sample at 350 x g for 15 min at room temperature. Transfer supernatant and store aliquots (120 µL each) at -20 °C until use.

5.5. Immediately before *in vivo* implantation, thaw the above aliquot and mix 20 µL with 0.5 x 10^6 MSCs (from either 1.9 or 3.1.2.1) detached from standard plates using trypsin/EDTA, or collect from chitosan plates by flushing (with PBS/medium).

5.6. Add 6 µL of 10% calcium chloride ($CaCl_2$) to the remaining 100 µL of thawed plasma in a well of 96-well plate to activate the plasma and induce formation of a clot (activated conditioned plasma: ACP).

5.7. Mix cell suspension (20 µL) and ACP (100 µL) to form a clot (**Figure 6**). Place the clot within the patellar tendon defect created before closing the fascia of the stifle (see step 4.10.3).

6. Functional Outcome

6.1. Monitor rats twice a day for signs of pain, based on the rat grimace scale (RGS)[37,38] and swelling over the implantation sites.

Note: A scoring system (0-6) was developed to evaluate ambulatory function based on 3 activities, including timed hind limb standing with forelimbs supported (0-3), timed unassisted hind limb standing (0-2), and the ability to climb a 17-cm plastic cage wall (0-1) (**Table 1**).

6.2. Evaluate rats for the two hind limb standing activities in the morning and in the evening of each time point to calculate an average score.

6.3. Evaluate rats for the ability to successfully climb a 17-cm plastic cage wall with both hind limbs reaching the top.

7. Gross Appearance and Histopathology of the Patellar Tendon

7.1. Euthanize rats at 7 days (to evaluate inflammation) or 28 days (to evaluate tissue healing) post treatment by intracardial injection of pentobarbital (100 mg/kg) under anesthesia with 8 % sevoflurane and 2 L 100% oxygen delivered via mask.

7.2. Harvest patella-tendon-tibia tuberosity units by scalpel and scissors after euthanasia. Remove soft tissues and ligaments around the stifle, except for the patellar tendon.

7.3. Examine each specimen for gross appearance and thickening of the tendon (**Figure 7**).

7.4. Orient the specimen by placing a surgeon's knot of 5.0 Polydioxanone on the proximal and lateral aspect of the tendon. Fix each specimen in 10% neutral buffered formalin solution and obtain transverse sections (5 μm) from the mid-portion of each tendon.

7.5. Stain the sections using hematoxylin and eosin, and Masson's Trichrome staining following standard protocols.

7.6. Examine section to detect the presence of hematoma within the defect, as well as pathological changes such as inflammation.

7.7. Evaluate the histological score of sections using the previously published scoring system, based on collagen grade, degree of angiogenesis, and cartilage formation (**Table 2**)[39].

REPRESENTATIVE RESULTS:

In the current study, results are presented as mean ± SD (standard deviation). Cells were isolated from the umbilical cords of 6 mares, and percentage of isolated cell lines expressing each cell surface marker under standard or chitosan conditioning were compared with a Friedman test, as a non-parametric analysis of variance with repeated measures. For tendon defect model creation, 8 rats were used for 7 days post-surgery assessment and 12 rats were used for 28 days assessment. Results of functional outcomes are presented as mean ± SEM (standard error of the mean) and compared using the t-test. UCM was selected as a cellular source due to its abundance, ease of collection, and superior proliferation relative to other fetal adnexa sources[40]. Cells isolated from UCM cultured on standard plates maintained a fibroblast-like shape throughout the expansion. Cells formed spheroids when cultured on chitosan plate (**Figure 8**).

The majority of cells cultured under standard conditions expressed CD44 (98.6 ± 1.62%), CD90 (88.7 ± 3.04%), and CD105 (77.9 ± 6.84%), while expression of CD34 (0.07 ± 0.17%) and MHC II (1.33 ± 1.12%) were very low. Under conditioned culture, the expression levels of CD44 (97.0 ± 2.12%) and CD34 (1.13 ± 1.58%) did not differ from standard cultures, while expression levels of CD90 (33.3 ± 37.1%) and CD105 (54.0 ± 19.0%) decreased and MHC II (2.84 ± 0.98%) increased[35].

Following isolation and characterization of UCM-MSCs *in vitro*, the biological behavior of conditioned cells was compared to that of cells cultured under standard conditions in a bilateral

patellar tendon defect model in rats. Untreated defects in each rat served as internal controls. Post-operative swelling was minimal in all rats and resolved within 48 h. According to the RGS, none of the rats displayed signs of pain or distress such as orbital tightening, nose/cheek flattening, or ear/whisker changes. All rats consumed a normal range of 3-4 pellets or 15-20 grams of feed daily throughout the study. The total functional score, including assisted and unassisted hind limb standing as well as climbing scores was higher in normal rats compared to that of operated rats at 7 days ($n = 8$, $p < 0.0001$, **Table 3**). However, the total functional score returned to normal within 28 days after surgery ($n = 12$, $p = 0.78$). Therefore, rat bilateral patellar tendon defect models have been shown to be effective for limiting inter-individual variation and reducing the necessary number of animals without causing significant morbidity (**Video 1-5**).

About 37% of tendons collected at 28 days appeared markedly thickened (**Figure 7**). This thickening was equally distributed between empty and treated defects. Total histological scores increased with time in untreated defects ($n = 20$, $p = 0.0034$). When each component of the healing score was evaluated independently, the only parameter changing with time consisted of cartilage formation, which increased between 7 and 28 days ($n = 20$, $p < 0.0001$). Angiogenesis tended to increase with time ($p = 0.3$), but collagen formation did not differ ($p = 0.69$). Upon histological examination, inflammation was observed in all of the tendons' tissue sections examined at 7 days after surgery, regardless of the presence of treatment. A hematoma was present in all treated defects. Histological angiogenesis scores (**Table 2, Figure 9**) ranged from 0 to 1, suggesting moderate arteriole and capillary infiltration, while collagen grade scores (**Table 2, Figure 10**) ranged from 2 to 3 overall, suggesting moderate to extensive collagen formation. Cartilage formation scores (**Table 2, Figure 11**) ranged from 0 to 2 suggesting no cartilage formation, to moderate cartilage formation of 25% to 50% of the tendon section area. All histological figures are oriented with the left side as the anterior aspect, and the top as the medial aspect of the transverse section of the mid-portion of the tendon.

FIGURE AND TABLE LEGENDS:

Figure 1: Positioning of rats and preparation for aseptic surgery. Each rat was placed between two 0.5 L water bottles filled with warm water and covered with a cloth to maintain body temperature and position, while preventing skin injury. The extremities of each rat were taped to the table and its body was covered with bubble wrap.

Figure 2: Surgical model of patellar tendon defect (alignment). A 0.99 mm-diameter Kirschner wire is aligned against the tendon as a template to standardize the size of the defect in each limb.

Figure 3: Surgical model of patellar tendon defect (incisions). Two full-thickness incisions are made on each side of the Kirschner wire to isolate a central portion of the tendon.

Figure 4: Surgical model of patellar tendon defect (resection). The central section is resected proximally and distally, creating a defect matching the size of the Kirschner wire. Resected area is shown within dotted line box.

Figure 5: Post-operative appearance of operated stifles. Fascia was closed with a cruciate pattern and skin was closed with an intradermal pattern.

Figure 6: Preparation of activated conditioned plasma for delivery of UCM-MSCs. Stem cells were suspended in conditioned plasma prior to activation. The resulting clot was inserted into patellar tendon defects.

Figure 7: Gross appearance of normal (C, D) and thickened (A, B) tendons. **A, C**: Posterior views; **B, D**: Lateral views; Block arrows identify the tibia and thin arrows identify the tendons.

Figure 8: Morphology of cells cultured on tissue culture plate under 19% oxygen level (standard group: A) and chitosan film under 5% oxygen level (conditioned group: B). Isolated cells were spindle shaped on standard group (**A**) and formed spheroids on conditioned group (**B**). Scale bar = 400 µm

Figure 9: **Representative light micrographs used for angiogenesis grading.** Following 7 days of healing, tendons with no treatment received a grade of 0 (**A**, **D**), whereas those with either conditioned cells (**C**, **F**) or standard cells (**B**, **E**) received a grade of 0.5 and 0, respectively. At 28 days, untreated tendons (**G**, **J**) received a grade of 0, whereas those with conditioned cells (**I**,**L**) or standard cells (**H**,**K**) received scores of 1.0 and 0.5, respectively. The arrows identify blood vessels present in the tendon sample. The arrows pointing to the blood vessels in 100x magnification correspond to the same arrows pointing to the blood vessels in the 400x magnification. Normal tendon tissue (**M**, **N**). Masson's trichrome stain (**A, B, C, G, H, I, M**); hematoxylin and eosin stain (**D, E, F, J, K, L, N**); bar = 100 µm (**A-N**).

Figure 10: Representative light micrographs used for collagen grading. Following 7 days of healing, tendons with no treatment received a grade of 2.5 (**A, D**) whereas those with treatment (**B, C, E, F**) received a grade of 3.0. At 28 days, untreated tendons (**G, J**) received a grade of 3.0, whereas those with conditioned cells (**I, L**) or standard cells (**H, K**) received scores of 1.0 and 3.0, respectively. The disorganization of the tendon fibers can be appreciated in 400x insets (**H, K**). Normal tendon tissue (**M, N**). Masson's trichrome stain (**A, B, C, G, H, I, M**); hematoxylin and eosin stain (**D, E, F, J, K, L, N**); bar = 100 µm (**A-N**).

Figure 11: **Representative light micrographs used for cartilage grading**. Following 7 days of healing, tendons with no treatment (**A, D**), those with either conditioned cells (**C, F**) or standard cells (**B, E**), all received a grade of 0. At 28 days, untreated tendons (**G, J**) received a grade of 1.0, whereas those with conditioned cells (**I, L**) or standard cells (**H, K**) received scores of 0 and 2.0, respectively. The arrows are pointing at chondrocytes present in the tendon sample. The arrows pointing to the chondrocytes in 100x magnification correspond to the same arrows pointing to the chondrocytes in the 400x magnification. Normal tendon tissue (**M, N**). Masson's trichrome stain (**A, B, C, G, H, I, M**); hematoxylin and eosin stain (**D, E, F, J, K, L, N**); bar = 100 µm (**A-N**).

Video 1: Evaluation of ambulatory function in rats. Timed unassisted hind limb standing (1 – 5 s: score 1) was observed 4 h post-operatively.

Video 2: Evaluation of ambulatory function in rats. Timed hind limb standing with forelimbs assisted (0 – 5 s: score 0) was noted 4 h post operatively.

Video 3: Evaluation of ambulatory function in rats. Timed unassisted hind limb standing (1 – 5 s: score 1), timed hind limb standing with forelimbs assisted (5 – 10 s: score 1) was noted 14 days post operatively.

Video 4: Evaluation of ambulatory function in rats. Timed hind limb standing with forelimbs assisted (10 – 15 s: score 2), without the ability to climb a 17-cm plastic cage wall (No climbing: score 0) was noted 27 days post operatively.

Video 5: Evaluation of ambulatory function in rats. Timed hind limb standing with forelimbs assisted (5 – 10 s: score 1), with the ability to climb a 17-cm plastic cage wall (Yes: score 1) was noted 14 days post operatively.

Table 1: Scoring system to evaluate ambulatory function in rats. A scoring system (0-6) was developed to evaluate ambulatory function based on 3 activities including timed hind limb standing with forelimbs supported (0-3), timed unassisted hind limb standing (0-2), and the ability to climb a 17-cm plastic cage wall (0-1).

Table 2: Histology scoring grades. Histological score of sections were graded based on collagen grade, degree of angiogenesis, and cartilage formation (adapted from Rosenbaum *et al.*[39])

Table 3: Functional scores of normal rats and untreated rats. Functional scores of normal rats and untreated rats 7 and 28 days postoperatively were graded. n = number of rats.

Supplementary Figure 1: Gating strategy and example of surface marker expression: Debris was excluded based on small FSC and SSC (**A**). Live cells were selected based on negative staining with 7-AAD detected by FL3 (**B**). Isotype matched control (**C**) was used as negative control to create a gate of CD44-FITC positive cells (**D**).

DISCUSSION:

Equine cells were selected for this project because we eventually intend to test candidate approaches in the management of natural tendinopathies in horses. Indeed, tendon injuries in horses are appealing as natural models of tendinopathy in man because of the biological similarity between the equine superficial digital flexor and Achilles tendon in humans[41]. The cell surface markers CD44, CD90, CD105, CD34, and MHC II were selected for immunophenotyping of cells, in accordance with the criteria recommended by the International Society for Cellular Therapy[42]. In a recent study, eqUCM-MSCs were positive for CD44 and negative for CD34 and MHC II, regardless of culture conditions. Cells cultured under standard conditions were also positive for CD90 and CD105, thereby meeting the criteria for MSCs in terms of expression of surface markers. Additionally, this study is the first report on the formation of spheroids when eqUCM-MSCs are cultured on chitosan film, confirming previous reports on human MSCs[19,20]. 3D

cell culture techniques have been extensively explored for decades aiming to create an environment resembling the physiological niche. Indeed, this study showed improved stemness gene expression levels of *Oct4*, *Sox2*, and *Nanog,* and improved differentiation potential, which is consistent with other reports[19,20]. Others reported improved immunomodulatory properties[43] and hyaline cartilage regeneration[44] using MSCs spheroids. Among various 3D culture techniques such as spinner flasks, rotating cell bioreactors, non-adherent plate, natural and synthetic matrices, chitosan films seem appealing for several reasons. This approach does not require expensive equipment and is cost-effective compared to non-adherent plates with synthetic matrices, since chitosan is a by-product of the seafood industry. Culturing cells on chitosan films is technically easy. Combined, these advantages would allow clinical application on a large scale[45].

The bilateral patellar tendon model proposed here appears acceptable in terms of morbidity. No complication was observed in a recent study study. We were especially concerned over the risk of stressful effects induced by defects large enough to allow detectable biomechanical and histological changes. These concerns prompted the selection of rats over mice for this study based on previous studies related to the size and maturity of the tendon for preclinical injury models. A 'window defect' or central-third patellar tendon defect has been described in rabbits[46] and rats[30,31] to study tendon healing and augmentation. The patellar tendon 'window defect' model has been found reproducible for studying tendon repair in rats with histology[31,39], biomechanical testing[30,31], and *ex vivo* fluorescence imaging[31]. In this study, the size of the defect was equivalent to the central third of the patellar tendon, and was standardized with a 0.99 mm-diameter Kirschner wire as a template. These dimensions were adequate to study tendon healing without causing post-operative rupture. Because of their larger anatomic size versus mice, rats can accommodate larger defects, improving the reproducibility of injury, treatment delivery, and measures of outcome.

The analgesia protocol administered to the rats in this study was effective in controlling post-operative pain, as assessed with the RGS[37,38]. This scoring system was selected here because it was previously validated as detecting post-operative behavioral changes reflecting pain in rats[37,38]. The RGS is based on signs relatively simple to identify, such as orbital tightening, nose/cheek flattening, and ear/whisker changes. Rats also maintained a normal food intake throughout this study, which further supports the efficacy of this analgesia protocol. Indeed, previous reports have found a correlation between post-operative pain and body weight changes in rats treated with non-steroidal anti-inflammatories, such as meloxicam[47]. This agent was selected in this study and preemptive administration was derived from studies in rats[37,48] and dogs[49], where the administration of anti-inflammatory agents immediately prior to surgery has been found to attenuate surgically induced pain. Function was assessed as an additional indicator of post-operative pain, using a scoring system designed to evaluate the use of both pelvic limbs. The three activities selected here provide a general assessment of the range of motion and willingness to bear weight on the pelvic limbs. This scoring system was derived from both static and dynamic functional recovery studies in rats[50,51] and was designed to compare the time course of the functional outcomes observed. Scores indicate that the bilateral tendon defect induced a temporary decrease in function at 7 days, with a return to normal within 28 days. The function

score appears more sensitive in detecting pain secondary to orthopedic conditions than the RGS. Similar functional tests have been used to evaluate tendon healing such as the Achilles Functional Index[28], paw and stride measures[51], or other macroscopic scoring systems[52].

This model was designed to reduce the number of animals enrolled in the study, while differentiating outcomes between untreated tendons and two stem cell-based treatments. The effects of the treatments tested in this study are discussed in another publication[36]. The model used here allowed detection of treatment differences through the use of an internal control in each rat, combined with non-destructive biomechanical testing of tendons at 28 days (data not presented here).

Activated conditioned plasma was selected because of its common use as a carrier for stem cells, biocompatibility, accessibility, and current clinical applications in the management of tendinopathies[53,54]. It may have contributed to the healing of treated tendons, but allowed local retention of stem cells, and it does not interfere with the comparison of treatment groups, since both included the same amount of activated conditioned plasma. The histological features of untreated tendons are consistent with previous descriptions of tendon healing, where necrotic tissue and disrupted collagen bundles are removed by phagocytosis and lytic enzymes by macrophages during the inflammation phase, which lasts up to 10 days post injury[54-56]. During the proliferative phase, cellular proliferation and vascularity of the repair site is greatest at 28 days after tendon repair[57,58]. We found a correlation between the apparent thickening of tendons, cross-sectional areas, and lower modulus of elasticity of specimens. Based on these results, the histological score seems to reflect tissue changes that may not be desirable and do not lead to biomechanical strength, such as disorganization of collagen fibers, angiogenesis, and chondrogenesis. In the future, the ability of this model to discriminate treatments based on histological characteristics may be improved by integrating additional criteria such as presence of tenocytes, extracellular matrix organization, proteoglycan content, and distribution of elastin fibers[52,59].

ACKNOWLEDGMENTS:
The authors would like to acknowledge Dr. Su, PhD, for her statistical analysis of the data. The authors also thank Dr. McClure, DVM, PhD DACLAM, for her advice on the anesthesia and pain management protocols used in the study. This project was supported by grants from Western University of Health Sciences Office of the Vice President for Research (12678v) and USDA Section 1433 funds (2090).

DISCLOSURES:
The authors have no conflict of interest to disclose.

REFERENCES:
1 Rossdale, P. D., Hopes, R., Digby, N. J. & offord, K. Epidemiological study of wastage among racehorses 1982 and 1983. *Vet Rec.* **116** (3), 66-69 (1985).
2 Black, D. A., Tucci, M., Puckett, A., Lawyer, T. & Benghuzzi, H. Strength of a new method of achilles tendon repair in the rat - biomed 2011. *Biomed Sci Instrum.* **47** 112-117 (2011).

3 Lake, S. P., Ansorge, H. L. & Soslowsky, L. J. Animal models of tendinopathy. *Disabil Rehabil.* **30** (20-22), 1530-1541, doi:10.1080/09638280701785460, (2008).

4 Frank, C. B. Ligament structure, physiology and function. *J Musculoskelet Neuronal Interact.* **4** (2), 199-201 (2004).

5 Godwin, E. E., Young, N. J., Dudhia, J., Beamish, I. C. & Smith, R. K. Implantation of bone marrow-derived mesenchymal stem cells demonstrates improved outcome in horses with overstrain injury of the superficial digital flexor tendon. *Equine Vet J.* **44** (1), 25-32, doi:10.1111/j.2042-3306.2011.00363.x, (2012).

6 Smith, R. K. *et al.* Beneficial effects of autologous bone marrow-derived mesenchymal stem cells in naturally occurring tendinopathy. *PLoS One.* **8** (9), e75697, doi:10.1371/journal.pone.0075697, (2013).

7 Fossett, E., Khan, W. S., Longo, U. G. & Smitham, P. J. Effect of age and gender on cell proliferation and cell surface characterization of synovial fat pad derived mesenchymal stem cells. *J Orthop Res.* **30** (7), 1013-1018, doi:10.1002/jor.22057, (2012).

8 Zaim, M., Karaman, S., Cetin, G. & Isik, S. Donor age and long-term culture affect differentiation and proliferation of human bone marrow mesenchymal stem cells. *Ann Hematol.* **91** (8), 1175-1186, doi:10.1007/s00277-012-1438-x, (2012).

9 Leychkis, Y., Munzer, S. R. & Richardson, J. L. What is stemness? *Stud Hist Philos Biol Biomed Sci.* **40** (4), 312-320, doi:10.1016/j.shpsc.2009.09.002, (2009).

10 VandeVord, P. J. *et al.* Evaluation of the biocompatibility of a chitosan scaffold in mice. *J Biomed Mater Res.* **59** (3), 585-590 (2002).

11 Griffon, D. J., Abulencia, J. P., Ragetly, G. R., Fredericks, L. P. & Chaieb, S. A comparative study of seeding techniques and three-dimensional matrices for mesenchymal cell attachment. *J Tissue Eng Regen Med.* **5** (3), 169-179, doi:10.1002/term.302, (2011).

12 Schwartz, Z., Griffon, D. J., Fredericks, L. P., Lee, H. B. & Weng, H. Y. Hyaluronic acid and chondrogenesis of murine bone marrow mesenchymal stem cells in chitosan sponges. *Am J Vet Res.* **72** (1), 42-50, doi:10.2460/ajvr.72.1.42, (2011).

13 Ragetly, G., Griffon, D. J. & Chung, Y. S. The effect of type II collagen coating of chitosan fibrous scaffolds on mesenchymal stem cell adhesion and chondrogenesis. *Acta Biomater.* **6** (10), 3988-3997, doi:10.1016/j.actbio.2010.05.016, (2010).

14 Ragetly, G. R., Griffon, D. J., Lee, H. B. & Chung, Y. S. Effect of collagen II coating on mesenchymal stem cell adhesion on chitosan and on reacetylated chitosan fibrous scaffolds. *J Mater Sci Mater Med.* **21** (8), 2479-2490, doi:10.1007/s10856-010-4096-3, (2010).

15 Ragetly, G. R. *et al.* Effect of chitosan scaffold microstructure on mesenchymal stem cell chondrogenesis. *Acta Biomater.* **6** (4), 1430-1436, doi:10.1016/j.actbio.2009.10.040, (2010).

16 Ragetly, G. R., Slavik, G. J., Cunningham, B. T., Schaeffer, D. J. & Griffon, D. J. Cartilage tissue engineering on fibrous chitosan scaffolds produced by a replica molding technique. *J Biomed Mater Res A.* **93** (1), 46-55, doi:10.1002/jbm.a.32514, (2010).

17 Slavik, G. J., Ragetly, G., Ganesh, N., Griffon, D. J. & Cunningham, B. T. A replica molding technique for producing fibrous chitosan scaffolds for cartilage engineering. *Journal of Materials Chemistry.* **17** (38), 4095-4101 (2007).

18 Griffon, D. J., Sedighi, M. R., Schaeffer, D. V., Eurell, J. A. & Johnson, A. L. Chitosan scaffolds: interconnective pore size and cartilage engineering. *Acta Biomater.* **2** (3), 313-320, doi:10.1016/j.actbio.2005.12.007, (2006).
19 Huang, G. S., Dai, L. G., Yen, B. L. & Hsu, S. H. Spheroid formation of mesenchymal stem cells on chitosan and chitosan-hyaluronan membranes. *Biomaterials.* **32** (29), 6929-6945, doi:10.1016/j.biomaterials.2011.05.092, (2011).
20 Cheng, N. C., Wang, S. & Young, T. H. The influence of spheroid formation of human adipose-derived stem cells on chitosan films on stemness and differentiation capabilities. *Biomaterials.* **33** (6), 1748-1758, doi:10.1016/j.biomaterials.2011.11.049, (2012).
21 Webster, R. A., Blaber, S. P., Herbert, B. R., Wilkins, M. R. & Vesey, G. The role of mesenchymal stem cells in veterinary therapeutics - a review. *N Z Vet J.* **60** (5), 265-272, doi:10.1080/00480169.2012.683377, (2012).
22 Khan, M. H., Li, Z. & Wang, J. H. Repeated exposure of tendon to prostaglandin-E2 leads to localized tendon degeneration. *Clin J Sport Med.* **15** (1), 27-33 (2005).
23 Sullo, A., Maffulli, N., Capasso, G. & Testa, V. The effects of prolonged peritendinous administration of PGE1 to the rat Achilles tendon: a possible animal model of chronic Achilles tendinopathy. *J Orthop Sci.* **6** (4), 349-357, doi:10.1007/s0077610060349, (2001).
24 van Schie, H. T. *et al.* Monitoring of the repair process of surgically created lesions in equine superficial digital flexor tendons by use of computerized ultrasonography. *Am J Vet Res.* **70** (1), 37-48, doi:10.2460/ajvr.70.1.37, (2009).
25 Schramme, M., Kerekes, Z., Hunter, S. & Labens, R. Mr imaging features of surgically induced core lesions in the equine superficial digital flexor tendon. *Vet Radiol Ultrasound.* **51** (3), 280-287 (2010).
26 Hast, M. W., Zuskov, A. & Soslowsky, L. J. The role of animal models in tendon research. *Bone Joint Res.* **3** (6), 193-202, doi:10.1302/2046-3758.36.2000281, (2014).
27 Warden, S. J. Animal models for the study of tendinopathy. *Br J Sports Med.* **41** (4), 232-240, doi:10.1136/bjsm.2006.032342, (2007).
28 Murrell, G. A. *et al.* Achilles tendon injuries: a comparison of surgical repair versus no repair in a rat model. *Foot Ankle.* **14** (7), 400-406 (1993).
29 Ozer, H. *et al.* [Effect of glucosamine chondroitine sulphate on repaired tenotomized rat Achilles tendons]. *Eklem Hastalik Cerrahisi.* **22** (2), 100-106 (2011).
30 Chan, B. P., Fu, S. C., Qin, L., Rolf, C. & Chan, K. M. Pyridinoline in relation to ultimate stress of the patellar tendon during healing: an animal study. *J Orthop Res.* **16** (5), 597-603, doi:10.1002/jor.1100160512, (1998).
31 Ni, M. *et al.* Tendon-derived stem cells (TDSCs) promote tendon repair in a rat patellar tendon window defect model. *J Orthop Res.* **30** (4), 613-619, doi:10.1002/jor.21559, (2012).
32 Orth, P., Zurakowski, D., Alini, M., Cucchiarini, M. & Madry, H. Reduction of sample size requirements by bilateral versus unilateral research designs in animal models for cartilage tissue engineering. *Tissue Eng Part C Methods.* **19** (11), 885-891, doi:10.1089/ten.TEC.2012.0699, (2013).
33 Kajikawa, Y. *et al.* Platelet-rich plasma enhances the initial mobilization of circulation-derived cells for tendon healing. *J Cell Physiol.* **215** (3), 837-845, doi:10.1002/jcp.21368, (2008).

34 Xu, W. *et al.* Human iPSC-derived neural crest stem cells promote tendon repair in a rat patellar tendon window defect model. *Tissue Eng Part A.* **19** (21-22), 2439-2451, doi:10.1089/ten.TEA.2012.0453, (2013).

35 Taguchi, T. *et al.* Influence of hypoxia on the stemness of umbilical cord matrix-derived mesenchymal stem cells cultured on chitosan films. *J Biomed Mat Res B: Appl Biomat.* n/a-n/a, doi:10.1002/jbm.b.33864, (2017).

36 Griffon, D. J. *et al.* Effects of Hypoxia and Chitosan on Equine Umbilical Cord-Derived Mesenchymal Stem Cells. *Stem Cells Int.* **2016** 2987140, doi:10.1155/2016/2987140, (2016).

37 Roughan, J. V. & Flecknell, P. A. Evaluation of a short duration behaviour-based post-operative pain scoring system in rats. *Eur J Pain.* **7** (5), 397-406, doi:10.1016/s1090-3801(02)00140-4, (2003).

38 Sotocinal, S. G. *et al.* The Rat Grimace Scale: a partially automated method for quantifying pain in the laboratory rat via facial expressions. *Mol Pain.* **7** 55, doi:10.1186/1744-8069-7-55, (2011).

39 Rosenbaum, A. J. *et al.* Histologic stages of healing correlate with restoration of tensile strength in a model of experimental tendon repair. *HSS J.* **6** (2), 164-170, doi:10.1007/s11420-009-9152-5, (2010).

40 Vidal, M. A., Walker, N. J., Napoli, E. & Borjesson, D. L. Evaluation of senescence in mesenchymal stem cells isolated from equine bone marrow, adipose tissue, and umbilical cord tissue. *Stem cells and development.* **21** (2), 273-283 (2011).

41 Patterson-Kane, J., Becker, D. & Rich, T. The pathogenesis of tendon microdamage in athletes: the horse as a natural model for basic cellular research. *J Compar Pathol.* **147** (2), 227-247 (2012).

42 Dominici, M. *et al.* Minimal criteria for defining multipotent mesenchymal stromal cells. The. *Cytotherapy.* **8** (4), 315-317, doi:10.1080/14653240600855905, (2006).

43 Bartosh, T. J. *et al.* Aggregation of human mesenchymal stromal cells (MSCs) into 3D spheroids enhances their antiinflammatory properties. *Proc Natl Acad Sci U S A.* **107** (31), 13724-13729, doi:10.1073/pnas.1008117107, (2010).

44 Zhang, K., Yan, S., Li, G., Cui, L. & Yin, J. In-situ birth of MSCs multicellular spheroids in poly(L-glutamic acid)/chitosan scaffold for hyaline-like cartilage regeneration. *Biomaterials.* **71** 24-34, doi:10.1016/j.biomaterials.2015.08.037, (2015).

45 Montanez-Sauri, S. I., Beebe, D. J. & Sung, K. E. Microscale screening systems for 3D cellular microenvironments: platforms, advances, and challenges. *Cellular and molecular life sciences : CMLS.* **72** (2), 237-249, doi:10.1007/s00018-014-1738-5, (2015).

46 Butler, D. L. *et al.* The use of mesenchymal stem cells in collagen-based scaffolds for tissue-engineered repair of tendons. *Nat Protoc.* **5** (5), 849-863, doi:10.1038/nprot.2010.14, (2010).

47 Brennan, M. P., Sinusas, A. J., Horvath, T. L., Collins, J. G. & Harding, M. J. Correlation between body weight changes and postoperative pain in rats treated with meloxicam or buprenorphine. *Lab Anim (NY).* **38** (3), 87-93, doi:10.1038/laban0309-87, (2009).

48 Ramon-Cueto, A., Cordero, M. I., Santos-Benito, F. F. & Avila, J. Functional recovery of paraplegic rats and motor axon regeneration in their spinal cords by olfactory ensheathing glia. *Neuron.* **25** (2), 425-435 (2000).

49 Arculus, S. L. Use of meloxicam as an analgesic in canine orthopaedic surgery. *Vet Rec.* **155** (24), 784 (2004).

50 Bervar, M. Video analysis of standing--an alternative footprint analysis to assess functional loss following injury to the rat sciatic nerve. *J Neurosci Methods.* **102** (2), 109-116 (2000).

51 Perry, S. M., Getz, C. L. & Soslowsky, L. J. Alterations in function after rotator cuff tears in an animal model. *J Shoulder Elbow Surg.* **18** (2), 296-304, doi:10.1016/j.jse.2008.10.008, (2009).

52 Stoll, C. *et al.* Healing parameters in a rabbit partial tendon defect following tenocyte/biomaterial implantation. *Biomaterials.* **32** (21), 4806-4815, doi:10.1016/j.biomaterials.2011.03.026, (2011).

53 Hankemeier, S. *et al.* Bone marrow stromal cells in a liquid fibrin matrix improve the healing process of patellar tendon window defects. *Tissue Eng Part A.* **15** (5), 1019-1030, doi:10.1089/ten.tea.2008.0046, (2009).

54 Silver, I. A. *et al.* A clinical and experimental study of tendon injury, healing and treatment in the horse. *Equine Vet J Suppl.* (1), 1-43 (1983).

55 Enwemeka, C. S. Inflammation, cellularity, and fibrillogenesis in regenerating tendon: implications for tendon rehabilitation. *Phys Ther.* **69** (10), 816-825 (1989).

56 Goldin, B., Block, W. D. & Pearson, J. R. Wound healing of tendon--I. Physical, mechanical and metabolic changes. *J Biomech.* **13** (3), 241-256 (1980).

57 Lyras, D. N. *et al.* The effect of platelet-rich plasma gel in the early phase of patellar tendon healing. *Arch Orthop Trauma Surg.* **129** (11), 1577-1582, doi:10.1007/s00402-009-0935-4, (2009).

58 Oshiro, W., Lou, J., Xing, X., Tu, Y. & Manske, P. R. Flexor tendon healing in the rat: a histologic and gene expression study. *J Hand Surg Am.* **28** (5), 814-823 (2003).

59 Visser, L. C., Arnoczky, S. P., Caballero, O. & Gardner, K. L. Evaluation of the use of an autologous platelet-rich fibrin membrane to enhance tendon healing in dogs. *Am J Vet Res.* **72** (5), 699-705, doi:10.2460/ajvr.72.5.699, (2011).

Figure 1

Click here to download Figure Figure 1.tif

Figure 2

Click here to download Figure Figure 2.tif

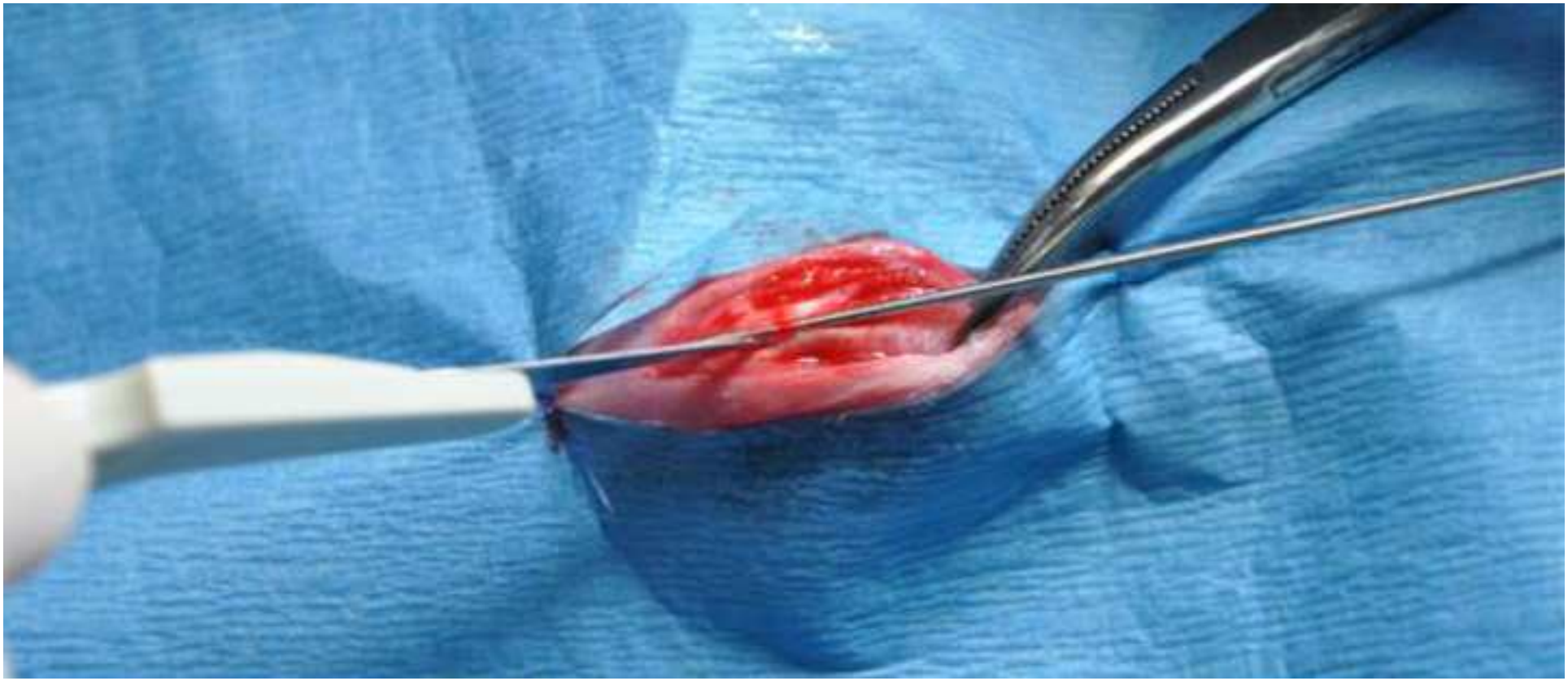

Figure 3

Click here to download Figure Figure 3.tif

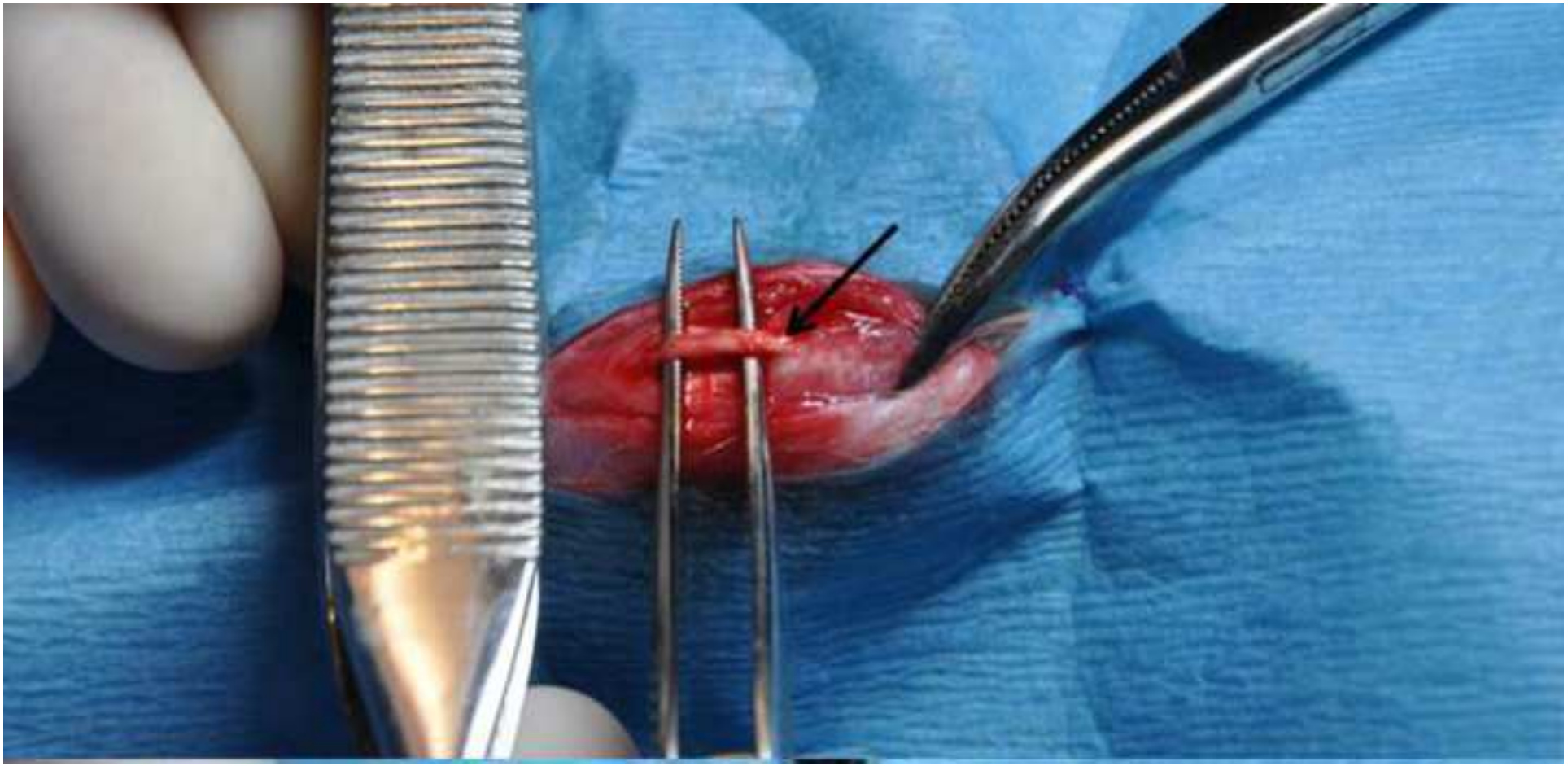

Figure 4

Click here to download Figure Figure 4 with dotted area.tif

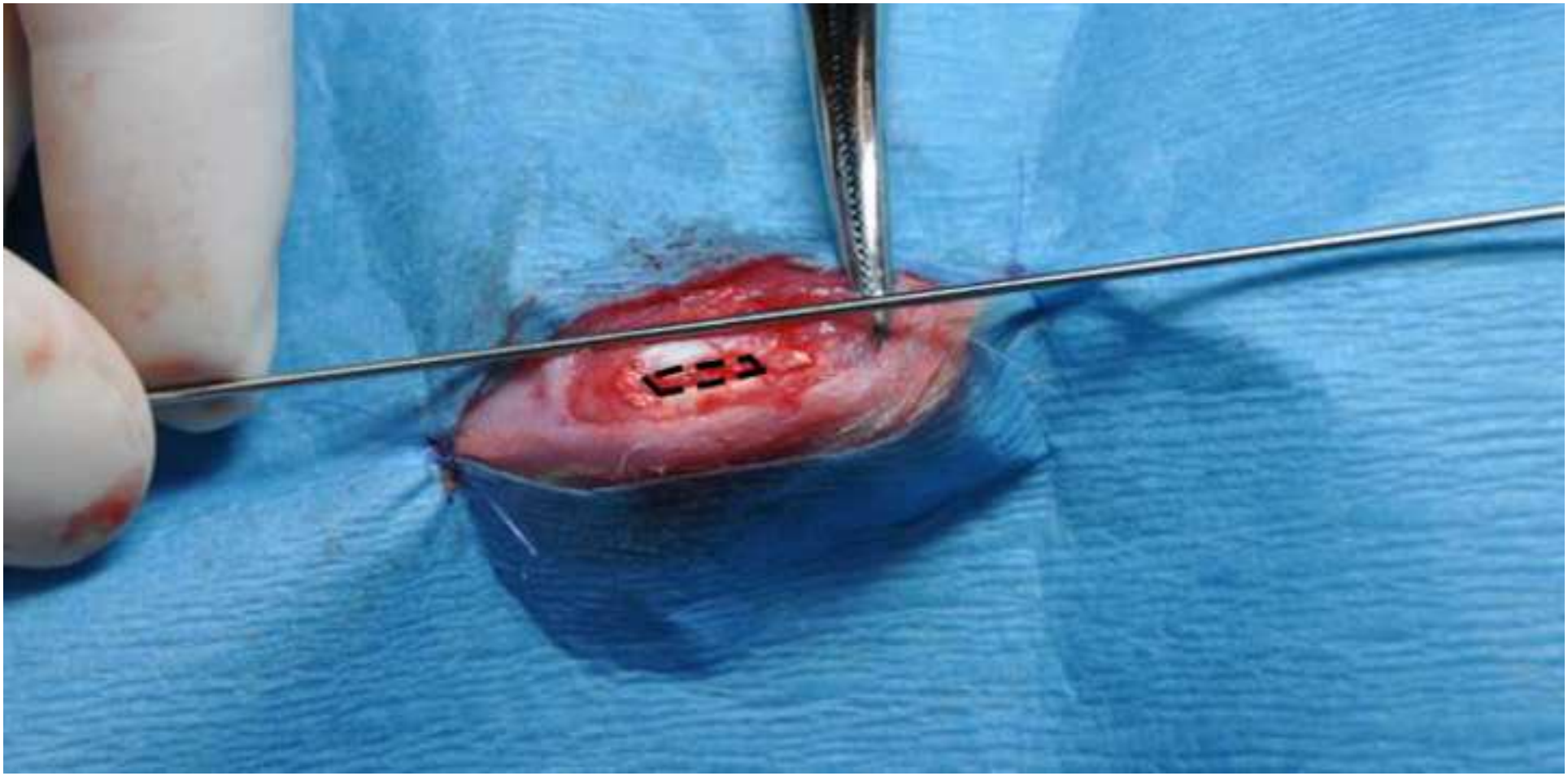

Figure 5

Click here to download Figure Figure 5.tif

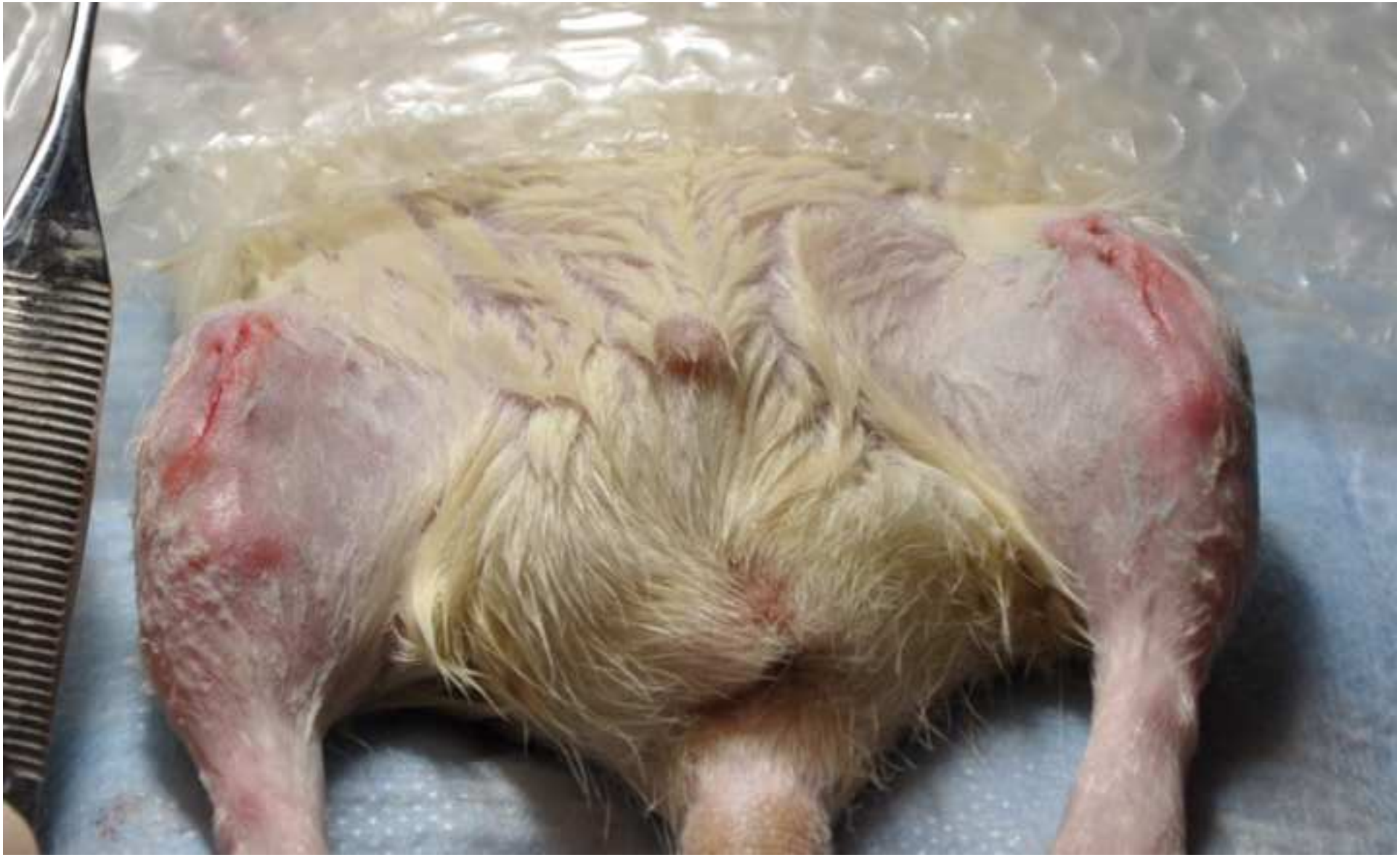

Figure 6

Click here to download Figure Figure 6.tif

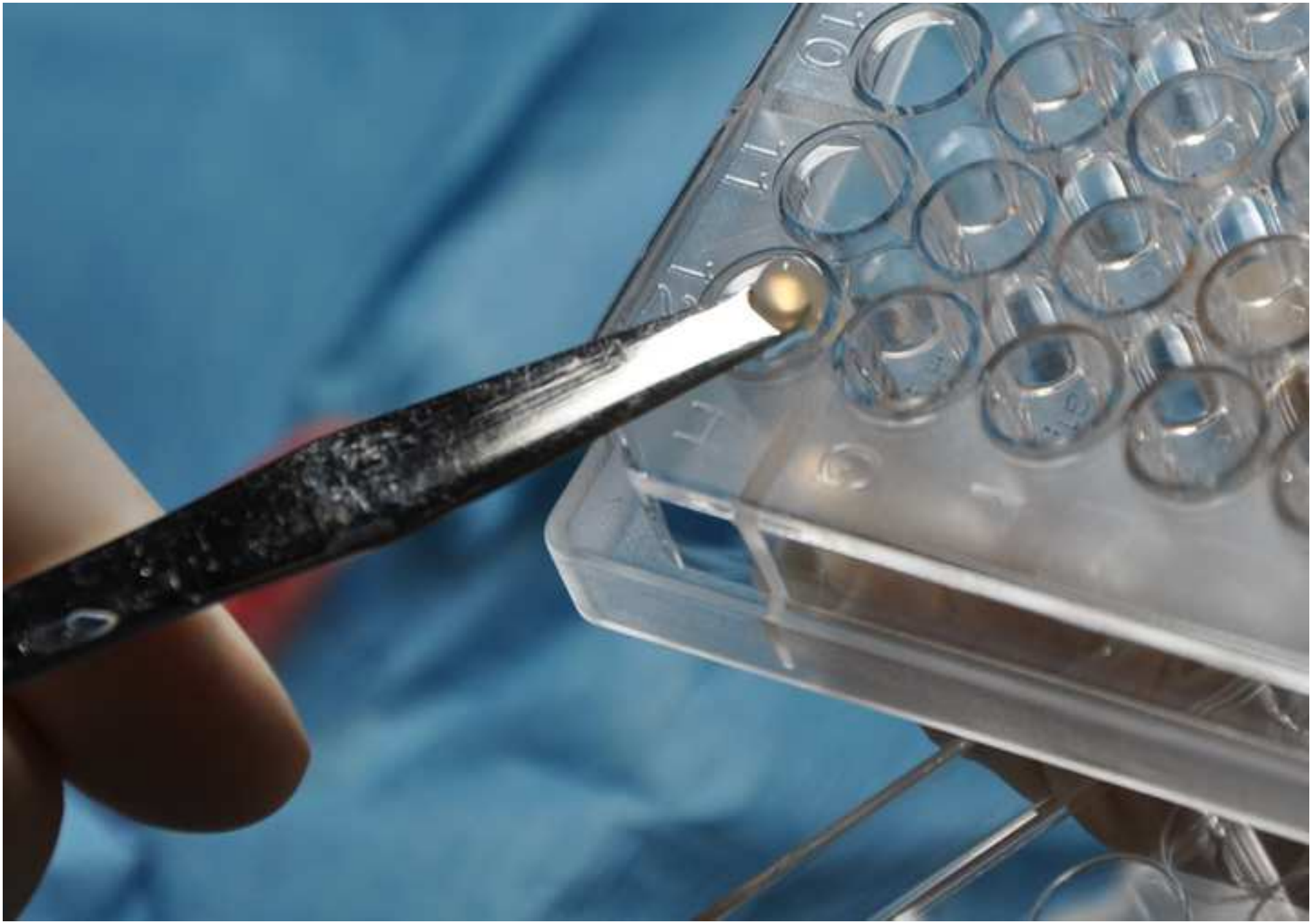

Figure 7

Click here to download Figure Figure 7.tif

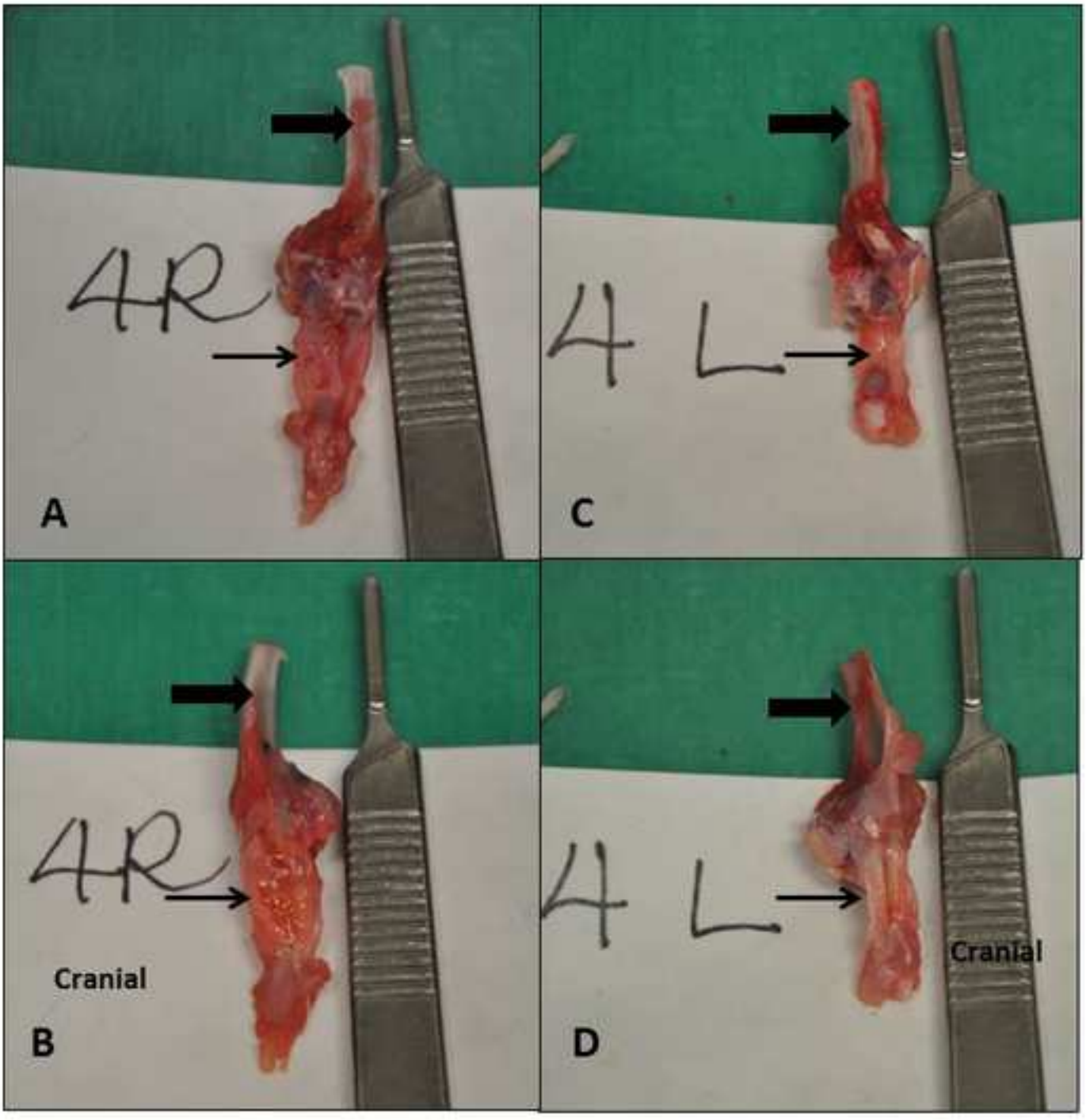

Figure 8

Click here to download Figure Figure 8 rotated.tif

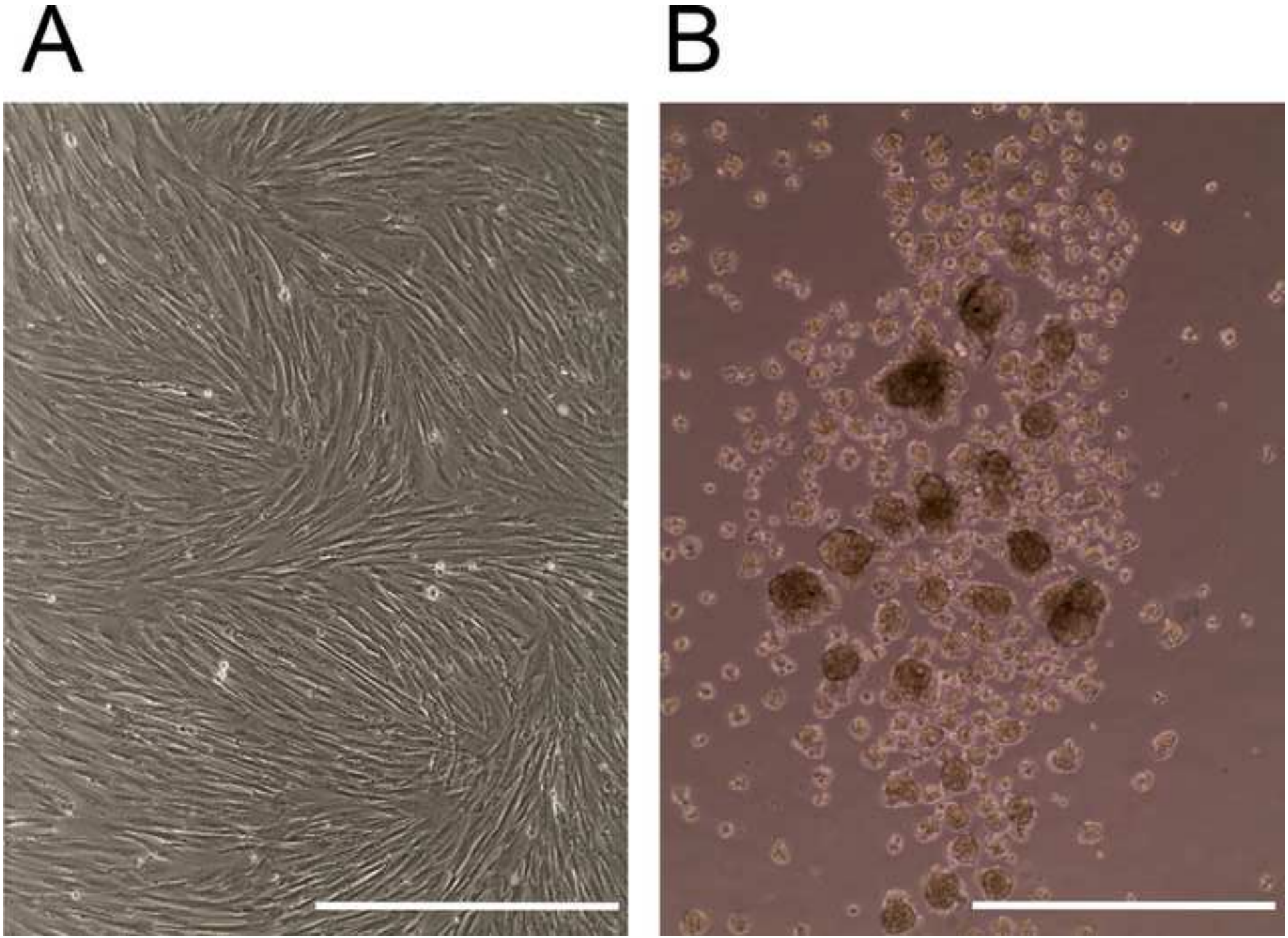

Figure 9

Click here to download Figure Figure 9.tif

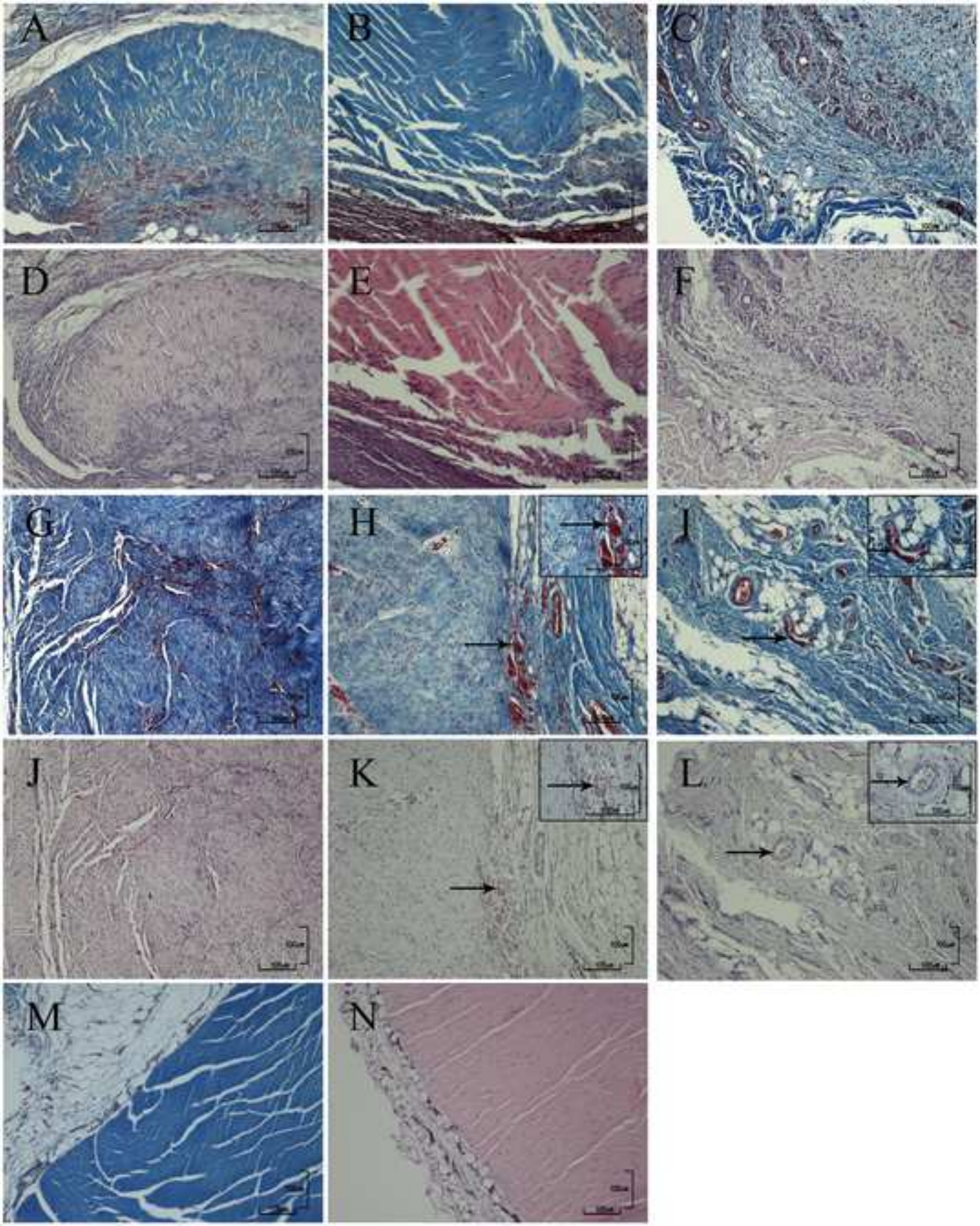

Figure 10

Click here to download Figure Figure 10.tif

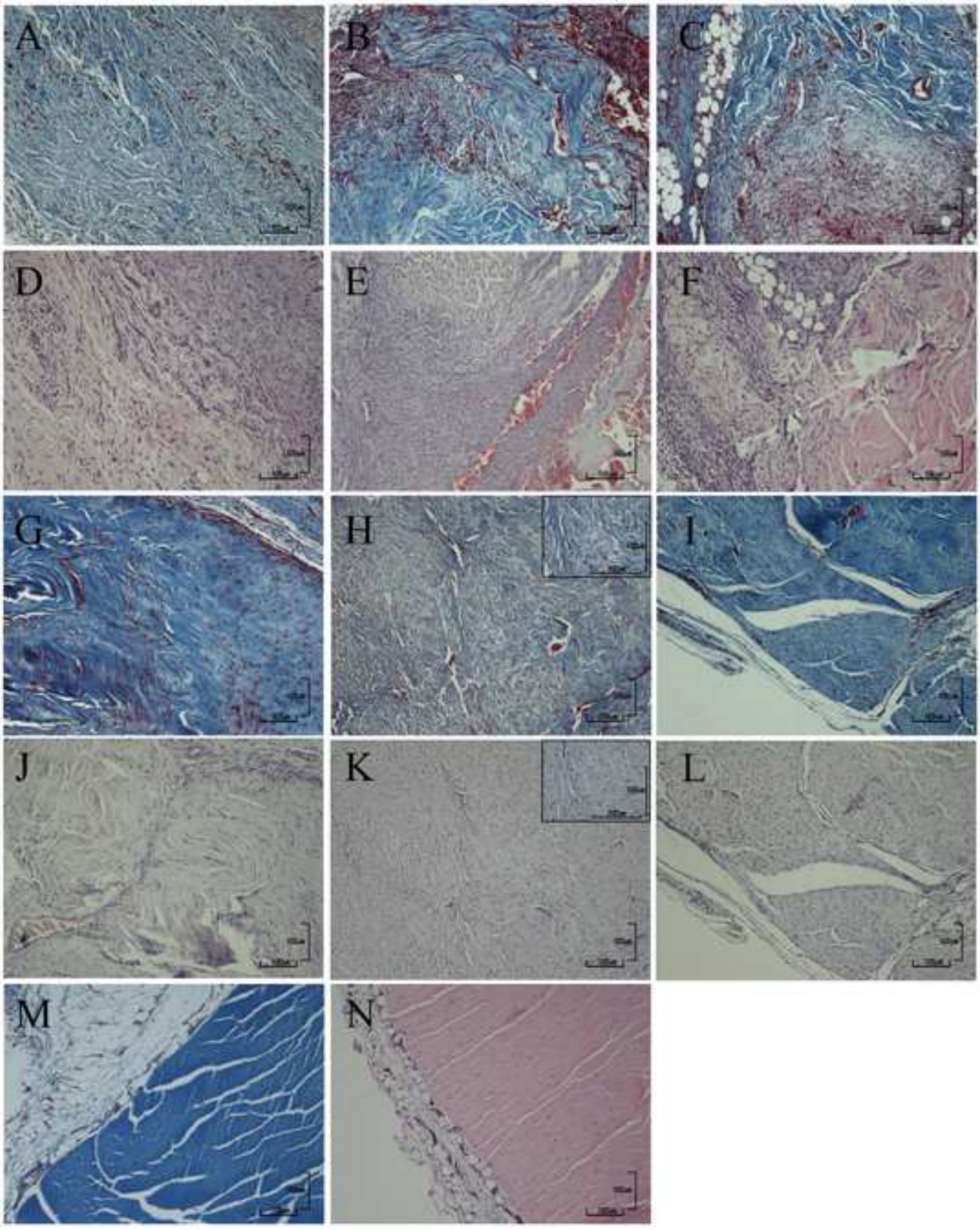

Figure 11

Click here to download Figure Figure 11.tif

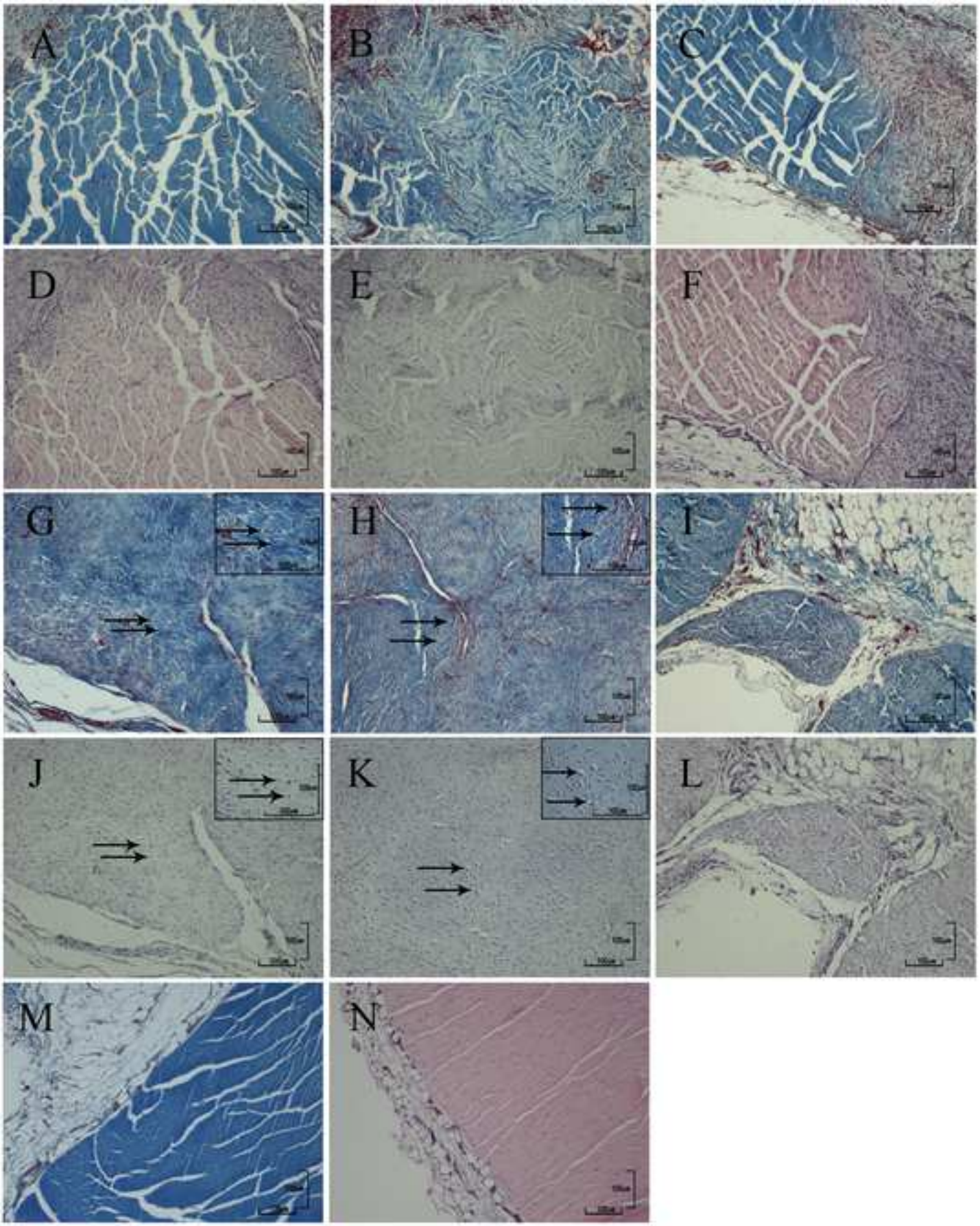

Video 1

Click here to access/download

Animated Figure (video and/or .ai figure files)

Video 1.mov

Video 2

Click here to access/download

Animated Figure (video and/or .ai figure files)

Video 2.mov

Video 3

Click here to access/download

Animated Figure (video and/or .ai figure files)

Video 3.mov

Video 4

Click here to access/download

Animated Figure (video and/or .ai figure files)

Video 4.MOV

Video 5

Click here to access/download

Animated Figure (video and/or .ai figure files)

Video 5.mov

Table

Functional Test	0	1	2	3	**Score**
Hind limb stand assisted	0-5 s	>5-10 s	>10-15 s	>15 s	
Hind limb stand unassisted	0-1 s	>1-5 s	>5 s		
Climbing ability	No	Yes			
				Total	

Table

Collagen grade
0
1
2
3
Degree of angiogenesis
0
1
2
Cartilage formation
0
1
2
3

Normal collagen oriented tangentially
Mild changes with collagen fibers less than 25% disorganized
Moderate changes with collagen fibers between 25% and 50% disorganized
Marked changes with collagen more than 50% disorganized
Moderate infiltration of tissue with arterioles
Presence of capillaries
No vasculature infiltration
No cartilage formation
Isolated hyaline cartilage nodules
Moderate cartilage formation of 25% to 50%
Extensive cartilage formation, more than 50% of the field involved

Table

Group	Mean ± SEM
Normal (n=3)	6.00 ± 0.48
7 days after surgery (n=8)	2.25 ± 0.30
28 days after surgery (n=12)	5.83 ± 0.24

Materials Table

Click here to download Materials Table Materials_JoVE.xls

Name of Material/ Equipment	Company	Catalog Number	Comments/Description
PBS 10X	Hyclone	SH30258.01	Consumable
Collagenase type IA	Worthington	LS004197	Consumable
DMEM low glucose	Hyclone	SH30021.FS	Consumable
Fetal Bovine Serum	Hyclone	SH30910.03	Consumable
Penicillin/Streptomycin 100X	Hyclone	SV30010	Consumable
Trypsin 0.25%	Hyclone	SH30042.01	Consumable
Accutase	Innovative Cell Technologies	AT104	Consumable
Trypan blue	Hyclone	SV30084.01	Consumable
Dimethyl Sulfoxide	Sigma	D2650	Consumable
Chitosan	Sigma	C3646	Consumable
Sodium Hydroxide	Sigma	S8045	Consumable
Bovine Serum Albumin	Hyclone	SH30574.01	Consumable
Round bottom polystyrene tube	Corning	149591A	Consumable
Mouse anti-horse CD44 (FITC)	AbD serotec	MCA1082F	Consumable
Mouse anti-rat CD90 (FITC)	AbD serotec	MCA47FT	Consumable
Mouse anti-horse MHC-II (FITC)	AbD serotec	MCA1085F	Consumable
Mouse IgG1 (FITC) - Isotype Control	AbD serotec	MCA928F	Consumable
Mouse monoclonal [SN6] to CD105 (FITC)	abcam	ab11415	Consumable
Mouse IgG1 (FITC) - Isotype Control	abcam	ab91356	Consumable
Mouse anti-human CD34 (FITC)	BD	BDB560942	Consumable
Mouse IdG1 kappa (FITC)	BD	BDB555748	Consumable
7-AAD	BD	BDB559925	Consumable
BD Accuri C6 Flow Cytometer	BD		Equipment
Vacutainer 5ml	Med Vet International	RED5.0	Consumable
Acid-citrate-dextrose	Sigma	C3821	Consumable
Calcium Chloride	Sigma	C5670	Consumable
Sevoflurane	JD Medical	60307-320-25	Consumable
Rats	Charles River	Strain code: 400	Experimental animal
Rat surgical kit	Harvard apparatus	728942	Equipment
Surgical Blade #15	MEDLINE	MDS15115	Consumable
Rat MD's Baytril (2 mg/Tablet), Rimadyl (2 mg/Tablet)	Bio Serv	F06801	Consumable

Polyglactin 910, 5-0	Ethicon	J436G	Consumable
Eosin alchol shandon	Thermo scientific	6766007	Consumable
Harris Hematoxylin	Thermo scientific	143907	Consumable

jove
JOURNAL OF VISUALIZED EXPERIMENTS

1 Alewife Center #200
Cambridge, MA 02140
tel. 617.945.9051
www.jove.com

ARTICLE AND VIDEO LICENSE AGREEMENT

Title of Article: Evaluation of stem cell therapies in a bilateral patellar Tendon injury...

Author(s): J Wyner, T Taguchi, J Cho, C Charavaryamath, D Griffon

Item 1 (check one box): The Author elects to have the Materials be made available (as described at http://www.jove.com/author) via: ☑ Standard Access ☐ Open Access

Item 2 (check one box):

☑ The Author is NOT a United States government employee.

☐ The Author is a United States government employee and the Materials were prepared in the course of his or her duties as a United States government employee.

☐ The Author is a United States government employee but the Materials were NOT prepared in the course of his or her duties as a United States government employee.

ARTICLE AND VIDEO LICENSE AGREEMENT

1. Defined Terms. As used in this Article and Video License Agreement, the following terms shall have the following meanings: **"Agreement"** means this Article and Video License Agreement; **"Article"** means the article specified on the last page of this Agreement, including any associated materials such as texts, figures, tables, artwork, abstracts, or summaries contained therein; **"Author"** means the author who is a signatory to this Agreement; **"Collective Work"** means a work, such as a periodical issue, anthology or encyclopedia, in which the Materials in their entirety in unmodified form, along with a number of other contributions, constituting separate and independent works in themselves, are assembled into a collective whole; **"CRC License"** means the Creative Commons Attribution-Non Commercial-No Derivs 3.0 Unported Agreement, the terms and conditions of which can be found at: http://creativecommons.org/licenses/by-nc-nd/3.0/legalcode; **"Derivative Work"** means a work based upon the Materials or upon the Materials and other pre-existing works, such as a translation, musical arrangement, dramatization, fictionalization, motion picture version, sound recording, art reproduction, abridgment, condensation, or any other form in which the Materials may be recast, transformed, or adapted; **"Institution"** means the institution, listed on the last page of this Agreement, by which the Author was employed at the time of the creation of the Materials; **"JoVE"** means MyJove Corporation, a Massachusetts corporation and the publisher of *The Journal of Visualized Experiments;* **"Materials"** means the Article and / or the Video; **"Parties"** means the Author and JoVE; **"Video"** means any video(s) made by the Author, alone or in conjunction with any other parties, or by JoVE or its affiliates or agents, individually or in collaboration with the Author or any other parties, incorporating all or any portion of the Article, and in which the Author may or may not appear.

2. Background. The Author, who is the author of the Article, in order to ensure the dissemination and protection of the Article, desires to have the JoVE publish the Article and create and transmit videos based on the Article. In furtherance of such goals, the Parties desire to memorialize in this Agreement the respective rights of each Party in and to the Article and the Video.

3. Grant of Rights in Article. In consideration of JoVE agreeing to publish the Article, the Author hereby grants to JoVE, subject to **Sections 4** and **7** below, the exclusive, royalty-free, perpetual (for the full term of copyright in the Article, including any extensions thereto) license (a) to publish, reproduce, distribute, display and store the Article in all forms, formats and media whether now known or hereafter developed (including without limitation in print, digital and electronic form) throughout the world, (b) to translate the Article into other languages, create adaptations, summaries or extracts of the Article or other Derivative Works (including, without limitation, the Video) or Collective Works based on all or any portion of the Article and exercise all of the rights set forth in (a) above in such translations, adaptations, summaries, extracts, Derivative Works or Collective Works and (c) to license others to do any or all of the above. The foregoing rights may be exercised in all media and formats, whether now known or hereafter devised, and include the right to make such modifications as are technically necessary to exercise the rights in other media and formats. If the "Open Access" box has been checked in **Item 1** above, JoVE and the Author hereby grant to the public all such rights in the Article as provided in, but subject to all limitations and requirements set forth in, the CRC License.

4. Retention of Rights in Article. Notwithstanding the exclusive license granted to JoVE in **Section 3** above, the Author shall, with respect to the Article, retain the non-exclusive right to use all or part of the Article for the non-commercial purpose of giving lectures, presentations or teaching classes, and to post a copy of the Article on the Institution's website or the Author's personal website, in each case provided that a link to the Article on the JoVE website is provided and notice of JoVE's copyright in the Article is included. All non-copyright intellectual property rights in and to the Article, such as patent rights, shall remain with the Author.

5. Grant of Rights in Video – Standard Access. This **Section 5** applies if the "Standard Access" box has been checked in **Item 1** above or if no box has been checked in **Item 1** above. In consideration of JoVE agreeing to produce, display or otherwise assist with the Video, the Author hereby acknowledges and agrees that, Subject to **Section 7** below, JoVE is and shall be the sole and exclusive owner of all rights of any nature, including, without limitation, all copyrights, in and to the Video. To the extent that, by law, the Author is deemed, now or at any time in the future, to have any rights of any nature in or to the Video, the Author hereby disclaims all such rights and transfers all such rights to JoVE.

6. Grant of Rights in Video – Open Access. This **Section 6** applies only if the "Open Access" box has been checked in **Item 1** above. In consideration of JoVE agreeing to produce, display or otherwise assist with the Video, the Author hereby grants to JoVE, subject to **Section 7** below, the exclusive, royalty-free, perpetual (for the full term of copyright in the Article, including any extensions thereto) license (a) to publish, reproduce, distribute, display and store the Video in all forms, formats and media whether now known or hereafter developed (including without limitation in print, digital and electronic form) throughout the world, (b) to translate the Video into other languages, create adaptations, summaries or extracts of the Video or other Derivative Works or Collective Works based on all or any portion of the Video and exercise all of the rights set forth in (a) above in such translations, adaptations, summaries, extracts, Derivative Works or Collective Works and (c) to license others to do any or all of the above. The foregoing rights may be exercised in all media and formats, whether now known or hereafter devised, and include the right to make such modifications as are technically necessary to exercise the rights in other media and formats. For any Video to which this Section 6 is applicable, JoVE and the Author hereby grant to the public all such rights in the Video as provided in, but subject to all limitations and requirements set forth in, the CRC License.

7. Government Employees. If the Author is a United States government employee and the Article was prepared in the course of his or her duties as a United States government employee, as indicated in **Item 2** above, and any of the licenses or grants granted by the Author hereunder exceed the scope of the 17 U.S.C. 403, then the rights granted hereunder shall be limited to the maximum rights permitted under such statute. In such case, all provisions contained herein that are not in conflict with such statute shall remain in full force and effect, and all provisions contained herein that do so conflict shall be deemed to be amended so as to provide to JoVE the maximum rights permissible within such statute.

8. Likeness, Privacy, Personality. The Author hereby grants JoVE the right to use the Author's name, voice, likeness, picture, photograph, image, biography and performance in any way, commercial or otherwise, in connection with the Materials and the sale, promotion and distribution thereof. The Author hereby waives any and all rights he or she may have, relating to his or her appearance in the Video or otherwise relating to the Materials, under all applicable privacy, likeness, personality or similar laws.

9. Author Warranties. The Author represents and warrants that the Article is original, that it has not been published, that the copyright interest is owned by the Author (or, if more than one author is listed at the beginning of this Agreement, by such authors collectively) and has not been assigned, licensed, or otherwise transferred to any other party. The Author represents and warrants that the author(s) listed at the top of this Agreement are the only authors of the Materials. If more than one author is listed at the top of this Agreement and if any such author has not entered into a separate Article and Video License Agreement with JoVE relating to the Materials, the Author represents and warrants that the Author has been authorized by each of the other such authors to execute this Agreement on his or her behalf and to bind him or her with respect to the terms of this Agreement as if each of them had been a party hereto as an Author. The Author warrants that the use, reproduction, distribution, public or private performance or display, and/or modification of all or any portion of the Materials does not and will not violate, infringe and/or misappropriate the patent, trademark, intellectual property or other rights of any third party. The Author represents and warrants that it has and will continue to comply with all government, institutional and other regulations, including, without limitation all institutional, laboratory, hospital, ethical, human and animal treatment, privacy, and all other rules, regulations, laws, procedures or guidelines, applicable to the Materials, and that all research involving human and animal subjects has been approved by the Author's relevant institutional review board.

10. JoVE Discretion. If the Author requests the assistance of JoVE in producing the Video in the Author's facility, the Author shall ensure that the presence of JoVE employees, agents or independent contractors is in accordance with the relevant regulations of the Author's institution. If more than one author is listed at the beginning of this Agreement, JoVE may, in its sole discretion, elect not take any action with respect to the Article until such time as it has received complete, executed Article and Video License Agreements from each such author. JoVE reserves the right, in its absolute and sole discretion and without giving any reason therefore, to accept or decline any work submitted to JoVE. JoVE and its employees, agents and independent contractors shall have

jove JOURNAL OF VISUALIZED EXPERIMENTS
1 Alewife Center #200
Cambridge, MA 02140
tel. 617.945.9051
www.jove.com

ARTICLE AND VIDEO LICENSE AGREEMENT

full, unfettered access to the facilities of the Author or of the Author's institution as necessary to make the Video, whether actually published or not. JoVE has sole discretion as to the method of making and publishing the Materials, including, without limitation, to all decisions regarding editing, lighting, filming, timing of publication, if any, length, quality, content and the like.

11. Indemnification. The Author agrees to indemnify JoVE and/or its successors and assigns from and against any and all claims, costs, and expenses, including attorney's fees, arising out of any breach of any warranty or other representations contained herein. The Author further agrees to indemnify and hold harmless JoVE from and against any and all claims, costs, and expenses, including attorney's fees, resulting from the breach by the Author of any representation or warranty contained herein or from allegations or instances of violation of intellectual property rights, damage to the Author's or the Author's institution's facilities, fraud, libel, defamation, research, equipment, experiments, property damage, personal injury, violations of institutional, laboratory, hospital, ethical, human and animal treatment, privacy or other rules, regulations, laws, procedures or guidelines, liabilities and other losses or damages related in any way to the submission of work to JoVE, making of videos by JoVE, or publication in *JoVE* or elsewhere by JoVE. The Author shall be responsible for, and shall hold JoVE harmless from, damages caused by lack of sterilization, lack of cleanliness or by contamination due to the making of a video by JoVE its employees, agents or independent contractors. All sterilization, cleanliness or decontamination procedures shall be solely the responsibility of the Author and shall be undertaken at the Author's expense. All indemnifications provided herein shall include JoVE's attorney's fees and costs related to said losses or damages. Such indemnification and holding harmless shall include such losses or damages incurred by, or in connection with, acts or omissions of JoVE, its employees, agents or independent contractors.

12. Fees. To cover the cost incurred for publication, JoVE must receive payment before production and publication the Materials. Payment is due in 21 days of invoice. Should the Materials not be published due to an editorial or production decision, these funds will be returned to the Author. Withdrawal by the Author of any submitted Materials after final peer review approval will result in a US$1,200 fee to cover pre-production expenses incurred by JoVE. If payment is not received by the completion of filming, production and publication of the Materials will be suspended until payment is received.

13. Transfer, Governing Law. This Agreement may be assigned by JoVE and shall inure to the benefits of any of JoVE's successors and assignees. This Agreement shall be governed and construed by the internal laws of the Commonwealth of Massachusetts without giving effect to any conflict of law provision thereunder. This Agreement may be executed in counterparts, each of which shall be deemed an original, but all of which together shall be deemed to me one and the same agreement. A signed copy of this Agreement delivered by facsimile, e-mail or other means of electronic transmission shall be deemed to have the same legal effect as delivery of an original signed copy of this Agreement.

A signed copy of this document must be sent with all new submissions. Only one Agreement required per submission.

CORRESPONDING AUTHOR:

Name: Dominique Griffon

Department: College of Veterinary Medicine

Institution: Western University of Health Sciences

Article Title: Evaluation of stem cell therapies in a labrador ...

Signature: 

Date: 6/13/17

Please submit a signed and dated copy of this license by one of the following three methods:

1) Upload a scanned copy of the document as a pfd on the JoVE submission site;
2) Fax the document to +1.866.381.2236;
3) Mail the document to JoVE / Attn: JoVE Editorial / 1 Alewife Center #200 / Cambridge, MA 02139

For questions, please email submissions@jove.com or call +1.617.945.9051

Aug 30th, 2017

Dear Dr. DSouza:

We would like to thank the reviewers for their thorough review of our manuscript entitled “Evaluation of stem cell therapies in a bilateral patellar tendon injury model in rats” (JoVE56810). Their comments were well-taken and constructive.

In the revised manuscript, we incorporated the reviewer’s comments. A detailed response to the reviewer’s comments is provided below.

We believe that the revised manuscript is much improved and will be of great interest to the readers of Journal of Visualized Experiments and the wider scientific community. We are looking forward to hearing from you soon.

Best regards,

Dominique Griffon, DVM, PhD.

1. Please include at least six keywords/phrases.

   Sixth keyword are added.

2. 2.10 Should be made into a note.

   It was made into a note part of 2.9.

3. 1.1: Mention the animal type/strain used.

   Pregnant mare. No particular strain noted.

4. 1.4: Do you use a microscope.

   No, anatomical feature of each component was identified by gross appearance.

5. 3.1.1.1: Is this done on the plates from 2.9?

   No, as indicated earlier in the text, it is explanation on how to treat cells in standard plates. Anyone who has done cell culture should be able to understand what this sentence is talking about. If needed, we can add "From step 1.14".

6. 3.1.2.1: How do you collect/handle the spheroids? Mention pipette tip size if relevant.

   The sentences were changed and more details were added as shown below:
   "3.1.2.1. Collect all spheroids by aspirating medium using pipette with 1000 µL tip. Transfer collected medium into 15 mL conical tube. After collecting medium, wash well by adding 1 ml of PBS, and transfer washed PBS into same 15 ml conical tube."

7. 3.1.2.3: Mention pipette tip size if relevant.

   The sentences were changed and more details were added as shown below:
   "Add 500 µL of the cell dissociation reagent and incubate for 5-10 min at room temperature. Mix by pipetting using 1 ml tip until spheroids dissociate and are no longer visible."

8. 3.3.3: What are the final antibody concentrations?

The antibody concentration was not provided for the ones we purchased. Instead, the recommendation from manufacture was to add 10 micro litter per 1 million cells, as described in manuscript.

9. 3.3.8: Describe the gating scheme.

   The sentences were changed and more details were added as shown below:
   "3.3.8. Analyze stained cell samples by flow cytometer. Exclude debris by their smaller SSC and FSC, and identify viable cells with lower uptake of 7-AAD. Plot FL1 and FL2 on y- and x- axis, respectively. Use isotype control to create a gate above diagonal line. Measure percentage of positively stained cells in the area. Count at least 20000 events/sample."

10. Section 4: Please add a step to mention and describe anesthesia (with drug dosage etc).

    Our anesthesia protocol is disclosed:
    4.2. Anesthetize the rat with 8 % sevoflurane in 2 L 100 % oxygen delivered via mask, until disappearance of pinch-toe reflex in the induction chamber.
    4.3. Inject Meloxicam (1mg/kg) subcutaneously as preemptive analgesia.

    4.4. Place the rat between 2 0.5L water bottles filled with warm water and covered with a cloth to maintain body temperature and position, while preventing skin injury. Tape each extremity to the table with tape. To reduce risk of hypothermia, cover the body with bubble wrap, (Figure 1).

    4.5. Maintain anesthesia with continuous flow of 5 % sevoflurane in 1 L 100 % oxygen mixture via nose cone with the animal on dorsal recumbency on water heating pad.

11. 4.1: Mention animal strain, age, sex, weight.

    There is description on animal strain, age, sex, weight:
    "Collect 5 mL blood by cardiac puncture from the anesthetized Sprague-Dawley rat (adult male, 4-5 months old, body weight 350-375 g), in a 5 mL syringe with 20 gauge needle containing 1 mL of acid-citrate-dextrose (5:1 v/v). "

12. 4.5: "A clot will form, retaining cells at the surgical site." This is confusing, isn't this in the suspension? Where does the surgical site feature here?

    Cell suspension will be gel-like clot due to mixture with 100 micro litter of ACP. The surgical site is the central portion of patella removed.

13. 4.5: Please mention the dissection steps, how is the tendon exposed? Mention surgical tools used.

    The tendon is immediately visible once the skin is incised.
    Surgical approach and tools used are described in section 5. 7-8:
    "4.8. Incise the skin with a #15 scalpel blade in a proximal to distal direction, on the craniomedial aspect of the stifle. The incision starts about 1 cm proximal to the level of the patella and extends approximately 5 mm distal to the tibial tubercle.

    4.9. Reflect the skin to expose the patellar tendon by freeing the underlying subcutaneous tissue with a #15 scalpel blade."

14. Section 4 should like appear after Section 5 for clarity.

    Order of section 4 and 5 were switched.

15. 5.3: What is the purpose of the bubble wrap?

    It was used to prevent hypothermia. Amended

16. 5.4: With scalpel?

17. 5.10: When is the clot (4.5) placed in the defect? How many days after the surgery in section 5?

    Clot was placed after creating window defect in patellar tendon. The sentence was changed accordingly:
    "5.7. Mix cell suspension (20 µL) and ACP (100 µL) to form a clot (Figure 6). Place the clot within the patellar tendon defect created before closing the fascia of the stifle."

18. 5.12 should likely appear before 5.11.

    The order of 5.11 and 5.12 was switched.

19. 7.1: Mention anesthesia dosage.

    Sentence was changed accordingly:
    "*Euthanize rats at 7 days (to evaluate inflammation) or 28 days (to evaluate tissue healing) post treatment by intracardial injection of pentobarbital (100 mg/kg) under anesthesia with 8 % sevoflurane and 2 L 100 % oxygen delivered via mask."*

20. 1.7,1.8,1.9 should be highlighted for continuity.

    These steps have been highlighted.

21. Section 3: Antibody incubation steps should be highlighted.

    Section 3. 3. 3 (antibody incubation step) was highlighted.

22. Please specify the format of quantitative results presented, for example, was mean ± standard deviation used? Mention sample sizes. Please mention the statistical tests performed.

    The sentences were changed and more details were added as shown below:
    "In the current study, results are presented as mean ± SD (standard deviation). Cells were isolated from umbilical cord of 6 mares and percentage of isolated cell lines expressing each cell surface marker under standard or chitosan conditioning were compared with a Friedman test, as non-parametric analysis of variance with repeated measures. For tendon defect model creation, 8 rats were used for 7 days post-surgery assessment and 12 rats were used for 28 days assessment. Results of functional outcome are presented as mean ± SEM (standard error of the mean) and compared using t-test. UCM was selected as cellular source due to its"

23. JoVE is unable to publish manuscripts containing commercial sounding language, including trademark or registered trademark symbols (TM/R) and the mention of company brand names before an instrument or reagent. Examples of commercial sounding language in your manuscript are Accutase.

    We replaced 'Accutase' with cell dissociation reagent (Accutase).

24. If your figures and tables are original and not published previously or you have already obtained figure permissions, please ignore this comment. If you are re-using figures from a previous publication, you must obtain explicit permission to re-use the figure from the previous publisher (this can be in the form of a letter from an editor or a link to the editorial policies that allows you to re-publish the figure). Please upload the text of the re-print permission (may be copied and pasted from an email/website) as a Word document to the Editorial Manager site in the "Supplemental files (as requested by JoVE)" section. Please also cite the figure appropriately in the figure legend, i.e. "This figure has been modified from [citation]."

    Figure 9 was adopted from previous publication. However, we have not obtained re-using permission. Additionally, the result of surface marker

expression is not essential in the article, as our focus is surgical procedure to create patellar tendon defect in rat. Therefore, figure 9 was removed, but results were kept in manuscript with proper citation.

Reviewer 1.

1. The authors used special staining techniques that did not allow them to evaluate Tendon repair. While Collagen is an important element of tendon structure but as stated by the authors Elastin fibers are the essential ECM component in the Tendon. Also, authors could use formation of Tenocytes as another indicator. Using markers for Elastin and tenocytes after cell therapy could be a useful tool to determine the degree of tendon repair. Adding this information will substantially increase the value of the paper.

   Thank you for these constructive suggestions on. The use of Masson's Trichrome and evaluation of Collagen was chosen because Collagen grade of repaired tissue was one of the criteria used in the histology scoring system used in our study. The system was adopted from a previously validated histological scoring for tendon repair, which had been shown to correlate with tensile strength[1]. Further studies with Elastin staining or other tendon markers such as Scx, Tnmd would certainly be beneficial in evaluating tendon healing and repair for future studies, listed at the end of our manuscript:
   "In the future, the ability of our model to discriminate treatments based on histological characteristics may be improved by integrating additional criteria such as presence of tenocytes, extracellular matrix organization, proteoglycan content, and distribution of elastin fibers[52,59]."

2. Authors used equine umbilical cord derived MSCs in an immune competent rat model. While xenogeneic transplantation of MSCs has been reported but the authors need to elaborate on this aspect. The inflammation described by the authors at day 7 post transplantation may be related to the immune response to the xenogeneic cells. Also, any information about the immune modulatory property of the equine umbilical cord derived MSC could be beneficial to the reader to understand justification of a xenogeneic test model. It is also important to know if this material is safe for clinical application. Are there adventitious agent concerns or allergic reaction considerations?

   Equine cells were selected in this project in view of clinical application in horses with tendon disease. This study was a pre-clinical trial. We believe equine MSCs did not elicit immune reaction in immune competent rat. There were inflammation in tendons at 7 days post-surgery in treated as

well as empty defects, as described in the sentence "Upon histological examination, inflammation was observed in all of the tendons tissue sections examined at 7 days after surgery, regardless of the presence of treatment." And the inflammation was not noted at 28 day post-surgery, when inflammation phase had passed and repair was transitioning from proliferative to remodeling phase. Report on in vivo implantation of equine UCM-MSCs is limited and there has been only one report using equine UCM-MSCs implanted in healthy horse muscle (allogenic)[2]. And our study was the first to report equine UCM-MSCs implanted in rat model. Regarding xenotransplantation, one review had reported 93.6% of studies using MSCs xenotransplantation had evidence of MSCs engrafted and functioned, and only 6.4% had evidence of failure to function[3]. So that safety of allogenic or even xenogenic transplantation have been extensively studied and established in MSCs treatment.
However, the scope of this manuscript is not to discuss the treatment or cells, but instead, to focus on the creation of a bilateral tendon injury model in rats, without significant morbidity. This model may be applied to any stem cell. Therefore, a discussion on immune privilege and immunomodulatory properties of MSCs was not included in this manuscript.

3. What is the conclusion with this study. Did the stem cell therapy assist with tendon healing? And was there a difference between the chitosan cultured cells and non-chitosan cultured cells? The authors describe disorganization of collagen fibers, angiogenesis and chondrocyte formation after cell therapy. These histological observations do not match the clinical improvement. Any explanation?

   The conclusion of this study has been clarified:
   "This bilateral patella tendon defect model controls inter-individual variation via creation of an internal control in each rat, was associated with acceptable morbidity and allowed detection of differences between untreated tendons and treatments."
   The effects of treatment are presented and discussed in another publication.[4]
   Regarding contradicting result of clinical improvement and increasing histological score, we only observed an increase in cartilage formation between day 7 and 28. Cartilage formation and fibrous scar tissue formation is one of the main problems why damaged tendon tend to re-injure at the site of cartilage or fibrous scar. We were able to observe functional improvement of animals and biomechanical properties of harvested tendon. However, treatment did not prevent cartilage formation, which is a natural response to tendon injury. We invite the reviewer to access the reference (open access) for further details.

4. The paper did not have a page number or line number so it makes it difficult to pin point to special section of the manuscript.

   Line numbering was added.

5. In second page, first paragraph of the introduction, the authors stated that they have previously observed the formation of spheroids and gave some references (11-16). Almost all these references point to promoted chondrogenic potential under this condition. Seeing chondrocyte and moderate cartilage formation in the tendon might also reflect that perhaps this system of culture is more suitable for cartilage repair than tendon repair. MSCs are multipotent and are known to differentiate into at least three cell types (chondrocyte, osteocyte and adipocyte). One of the big challenges in cell therapy is to hope the stem cells differentiate into the cell type that is surrounded. Fig.11, C and F contains some adipocytes. It is difficult to say if these are originated from the equine cells or are rat adipocytes. These points need to be stated and discussed in the revised manuscript.

   It is true that many spheroid formation of MSCs have been found to correlate with better chondrogenesis as stated in references. In addition, hypoxia conditioning is known to enhance chondrogenesis of MSCs[5,6]. Adipose tissue found in Fig. 11 C and F might be equine MSCs origin or rat native tissue. Interestingly, there appeared to be more adipocyte in tendon of conditioned cell treatment group. Therefore, it can be interpreted implanted MSCs differentiated to chondrocyte or adipocyte due to their multi-lineage differentiation capacity. However, all these evidences on differentiation capacity are in vitro phenomenon and there has been no answer to the question whether implanted MSCs indeed differentiated to desired lineage or not. MSCs might have functioned to improve healing by trophic factor release or immunomodulatory properties under acute inflammatory environment. It is very important and interesting to know what properties of MSCs contributed clinical improvement or biomechanical strength of tendon. However, the scope of this study was to investigate the effect of preconditioning on clinical outcome or biomechanical properties of repaired tendon, which has been discussed in previous publication[4]. Although further investigation on MSCs behavior after implantation is warranted, this issue was beyond our scope and therefore not included in the manuscript.

6. Protocol, 1.3. Trice is not a common English word. Please replace that with three times. 1.6. How much of the tissue is digested after 3-4h and on average how many cells per gram of the umbilical cord tissue is expected to obtain?

*The term thrice was replaced with three times throughout the manuscript. The number of isolated cells were not counted as we did not perform red blood lysis to minimize negative effect on MSCs. MSCs were selectively isolated using their plastic adherent property following 12 - 24 h incubation by medium change. However, we had used 12 – 15 g of tissue and SVF was seeded onto T25 flask, which then lead to 80 – 90 % confluence by day 7. As a reference, isolation of 10 – 50 * 10^3 cells/cm of umbilical cord from human is reported[7].*

7. Results, second page, second paragraph, the authors stated that rats recover after 28 days of transplantation. This is very fast as compared to tendon repair in the horse that takes months to occur. May be the size of the injury and the weight of animal or species differences are the reason for the fast recovery in rat as compared to slow recovery in horse. Using some references discussing the time require for full tendon recovery in horse could help the reader to understand the difference.

   We appreciate the suggestion to discuss on function recovery differences between species. It is very important to appreciate rat model we had created differ from horse model or patient in terms of weight or biomechanics. Indeed, functional recovery of rat model was relatively faster than horse patients and this might be due to light weight and lower load on injured tendon. Although not included in this manuscript, even functionally normal rats had lower biomechanical properties of tendon compared to normal rats' tendon. This suggest full recovery of tendon had not been achieved by day 28.
   The scope of this study was comparison of different treatments using small rodent model as proof-of-concept for the horse application. The results obtained by using this rat model may not be directly extrapolated to horse patients, but it is a robust model to test a new treatment before trial in larger animals, because small size and fast life cycle reduce the cost and time needed for study. Also we believe fast functional recovery is advantageous to observe difference in treatments' efficacy in short term. Therefore, species difference of tendon recovery was beyond our scope and not discussed in this manuscript.

8. Discussion, first page last three lines and the first line in the second page of discussion, the authors compare the spheroid with bioreactor and conclude that spheroid is a more cost effective for scale up manufacturing of MSCs. It is important for the reader to know how many cells can be grown on the spheroids as compared to bioreactor. This is debatable, as for scale-up patient therapy it becomes very demanding and labor intensive to handle so many culture dishes at a time.

   Bioreactor, ultra-low attachment culture plate, hanging drop method, chitosan film coated plate all forms spheroids. And spheroid size, number,

and cellular number growing within spheroids vary depending on initial cell number, medium properties, etc., but it is consistently observed cells proliferate much slower within spheroid independent of which method used. Therefore, spheroid formation itself is not suited for scale-up therapy of MSCs. Instead, as several study reported previously, spheroid formation has been found to improve properties of MSCs[4,8].
The advantage of chitosan film is low cost of the material itself due to the fact that chitosan is by-product of seafood industry. As discussed in the manuscript, other methods require either equipment to create specific condition (e.g. rotating reactor) or expensive coating of culture flask. On the other hand, chitosan film coating is easy and can coat any size of surface area, so that it is relatively easier when scale-up of spheroid formation is necessary. To make easier for readers to understand, the sentences were changed and more details were added as shown below: "Among various 3D culture techniques such as spinner flasks, rotating cell bioreactors, non-adherent plate, natural and synthetic matrices, chitosan film seems appealing because there is no necessity for expensive equipment, it is cost effective compared to non-adherent plate with synthetic matrices due to the fact that chitosan is by-product of seafood industry, and it is easy to change medium, which makes this technique suitable for scale-up patient therapy."

9. Figure legends. Fig 11. The arrows describing the blood vessels are in Fig 10. The statement describing the blood vessel belongs to Fig 10. It seems that Fig legends for Fig. 10 and Fig 11 need to be replaced.

   Figure legends 10 and 11 were switched and changes were made also in manuscript accordingly.

10. Could NSAID administration falsely improved ambulation and reduced pain post surgery? Also, could it have reduced the effectiveness of the MSCs?

    NSAIDs were administered to all rats in the study as a therapeutic dose for pain control. There is rather weak evidence to absolute contraindicate the use of NSAIDs in subjects that have had post-operative surgery. And NSAIDs definitely improved and reduced post-surgical pain, which then lead to no difference in functional score between standard and conditioned cell treatment group[4]. However, functional score was measured not to evaluate the difference of treatment group, but to prove creation of bilateral tendon injury does not cause significant morbidity by NSAIDs administration. Although there have been studies that NSAIDs may interfere with stem cells, such as effect on hematopoietic stem cells (HSCs) migration pattern[9], the exact mechanism behind the relationship of NSAIDs and MSCs is yet to be found.

11. The expression of some surface markers changed in the presence of Chitosan. What could be the meaning of these changes? Are the cells differentiating in culture? Although small and arguably negligible MHC-II increase, could this increase raise concern for an immune response with allogenic application in the clinic? Could this increase have been caused by the use of Chitosan from shellfish shells?

    It will be very interesting to investigate phenotypical change along with surface marker expression change. It is possible that those cells with different surface markers are differentiating within spheroids. There are reports on relationship with reduced CD90 and CD105 expression and enhance osteogenesis or adipogenesis[10,11]. However, this issue was also beyond our scope and we put emphasis on enhancement of stemness genes (Oct4, Sox2, Nanog) and biomechanical strength improvement[4]. Further investigation on surface marker expression change and differentiation caused by culturing on chitosan is warranted.
    As suggested by reviewer 1, slight increase of MHC II raise a concern to some extent. There is a report on mismatched haplotype of allogenic MSCs induced immune reaction, whereas MHC II negative MSCs suppressed immune reaction[12]. In the literature, MSCs which caused immune reaction expressed mostly above 50%, so that slight increase observed in our study may not elicit immune reaction upon allogenic application. However, it'll be beneficial for future allogenic application to investigate on threshold to cause immune reaction.

Reviewer 2.

1. The MSCs used for wounded rat tendon healing were isolated from mare placenta. Were any immunoreactions found in the rats caused by the mare MSCs? Because this is a kind of xenotransplantation. The healed tissue should be tested for anti-mare-MSCs antibodies, such as anti-rat collagen type I and anti-horse collagen type I antibodies. To demonstrate the healed tissue was from implantation of mare MSCs, not from rat self.

    There were inflammation from all injured tendon with or without MSCs treatment at day 7, which is not observed at day 28. And immune reaction associated with MSCs application was not observed in any tissue collected. Although collected tissue was not tested with α-horse or α-rat collagen type I Abs, the tracking of MSCs were performed by GFP expression of MSCs[4]. And presence of implanted MSCs were confirmed up to 28 days post-surgery. It'll be difficult to determine which MSCs from horse or rat deposited collagen type I and contributed to tendon healing. Yet, we were able to conclude that tendon with MSCs treatment had better biomechanical properties compared to tendon without treatment. Therefore, MSCs from horse contributed to tendon healing either by

differentiation, trophic factor, or immunomodulation. We appreciate very constructive suggestion on collagen staining as it will partly answer the question about what function of MSCs lead to improvement of biomechanical strength. This assay should be included in future study.

2. Fig. 2 shows that a water bottle was used for temperature keeping. I suggest using an electric blanket to instead of bottle (better control the temperature and convenient for operation).

   Given the short anesthetic surgical procedure, warm water bottles were used. We can absolutely substitute for an electric blanket, or a circulating warm water heating pad.

3. The picture in Fig. 3 is too small and it looks like the wire just past through the paratenon, not tendon. Please tell the thickness of the tissue above the wire (or provide a high-quality picture to see more details).

   Replaced - Figure 3 is a Tiff file at 1,600kb, which should suffice for online publication.
   The wire is placed on the center of tendon. The tendon measures about 3mm in width but the thickness estimated at 1-2mm. Details should be easier to see online as readers will be able to magnify images. In addition, a video will be provided. We are willing to let the photographer take additional pictures during the session, if the Editor finds it necessary.

4. The picture in Fig. 4 is not clear. It is difficult to find the wounds (too much blood). Please provide a larger picture shown the wound area.

   Replaced - Figure 4 is a Tiff file at 790kb. The central portion is clearly identified as the band of tissue positioned over the forceps and identified with an arrow.
   Details should be easier to see online as readers will be able to magnify images. In addition, a video will be provided. We are willing to let the photographer take additional pictures during the session, if the Editor finds it necessary.

5. Where is the defect in Figure 5? Please provide a high-quality picture and add an arrow to tell the wound area.

   Replaced- The Tiff file is 765kb
   Details should be easier to see online as readers will be able to magnify images. In addition, a video will be provided. We are willing to let the photographer take additional pictures during the session, if the Editor finds it necessary.

6. Why are right tendons bigger than left tendons shown in Figure 7?

The changes are consistent with postoperative inflammation, but we do not have evidence to explain this inconsistent finding. In Figure 7, two tendons from right hind limbs showed thickening. However, thickening of tendon was observed in both right and left limbs. Also there was no relationship between tendon thickening and presence of treatment. This was discussed in result section as shown below:
"About 37% of tendons collected at 28 days appeared markedly thickened (Figure 7). This thickening was equally distributed between empty and treated defects."

7. All the pictures should be larger so that the wound and treatment can be seen more clearly.

   Addressed above

8. The staining results on stem cell markers should be added in Figure 8.

   Due to the fact that we did not obtain permission to adopt Figure 9 (staining of stem cell markers) from previous publication and limited time frame, we removed Figure 9. However, the same result was left in result section with proper citation.

9. How were the results shown in Figure 9 obtained? By Flow cytometry? Or immunostaining? If the results were obtained by flow cytometry, please provide flow cytometry graph (or staining picture).

   Result of Figure 9 was obtained by flow cytometry. Scattered plot of flow cytometry is previously published and was excluded from this manuscript, because the focus of this manuscript was methodological explanation of surface marker expression from MSCs within spheroids and brief presentation of result. However, citation of our previous publication for surface marker expression level will aid in obtaining detailed information of flow cytometry data[13].

10. Figure 10: were these tissue sections from patellar tendons? Why is the organization of the collagen fibers so poor? The normal tendon sections with the same staining should be provided.

    These sections were from patellar tendons. It is unclear what caused the disorganization of collagen after surgery. The reason of disorganized collagen fibers is possibly due to change in biomechanical properties after surgery, such as dislocation of well aligned collagen toward central defect or change in direction of tensile stress moves through tendon. For comparison, the normal tendon histology was added to the figure 10,11, and 12 for comparison.

11. Figure 11: please indicate the wound area and the healed tendon area in each picture.

    In all the figure of histology including Figure 11, the images represented as empty or treated (A – L) shows only wound area because each images were approximately 800 x 600 µm and were not large enough to include both normal and wound area of tendon. Instead, images of normal tendon were added (M, N).

References

1 Rosenbaum, A. J. *et al.* Histologic stages of healing correlate with restoration of tensile strength in a model of experimental tendon repair. *HSS J.* **6** (2), 164-170, doi:10.1007/s11420-009-9152-5, (2010).

2 Dias, M. C. *et al.* Intramuscular Transplantation of Allogeneic Mesenchymal Stromal Cells Derived from Equine Umbilical Cord. *International Journal of Stem Cells.* **9** (2), 239-249, doi:10.15283/ijsc16011, (2016).

3 Li, J., Ezzelarab, M. B. & Cooper, D. K. C. DO MESENCHYMAL STEM CELLS FUNCTION ACROSS SPECIES BARRIERS? RELEVANCE FOR XENOTRANSPLANTATION. *Xenotransplantation.* **19** (5), 273-285, doi:10.1111/xen.12000, (2012).

4 Griffon, D. J. *et al.* Effects of Hypoxia and Chitosan on Equine Umbilical Cord-Derived Mesenchymal Stem Cells. *Stem Cells Int.* **2016** 2987140, doi:10.1155/2016/2987140, (2016).

5 Adesida, A. B., Mulet-Sierra, A. & Jomha, N. M. Hypoxia mediated isolation and expansion enhances the chondrogenic capacity of bone marrow mesenchymal stromal cells. *Stem Cell Res Ther.* **3** (2), 9, doi:10.1186/scrt100, (2012).

6 Buravkova, L. B., Andreeva, E. R., Gogvadze, V. & Zhivotovsky, B. Mesenchymal stem cells and hypoxia: where are we? *Mitochondrion.* **19 Pt A** 105-112, doi:10.1016/j.mito.2014.07.005, (2014).

7 Weiss, M. L. *et al.* Human umbilical cord matrix stem cells: preliminary characterization and effect of transplantation in a rodent model of Parkinson's disease. *Stem Cells.* **24** (3), 781-792, doi:10.1634/stemcells.2005-0330, (2006).

8 Hsu, S. H., Huang, G. S. & Feng, F. Isolation of the multipotent MSC subpopulation from human gingival fibroblasts by culturing on chitosan membranes. *Biomaterials.* **33** (9), 2642-2655, doi:10.1016/j.biomaterials.2011.12.032, (2012).

9 Hoggatt, J. *et al.* Differential Stem and Progenitor Cell Trafficking by Prostaglandin E(2). *Nature.* **495** (7441), 365-369, doi:10.1038/nature11929, (2013).

10 Moraes, D. A. *et al.* A reduction in CD90 (THY-1) expression results in increased differentiation of mesenchymal stromal cells. *Stem Cell Research & Therapy.* **7** (1), 97, doi:10.1186/s13287-016-0359-3, (2016).

11 Anderson, P., Carrillo-Gálvez, A. B., García-Pérez, A., Cobo, M. & Martín, F. CD105 (Endoglin)-Negative Murine Mesenchymal Stromal Cells Define a New Multipotent Subpopulation with Distinct Differentiation and Immunomodulatory Capacities. *PLoS ONE.* **8** (10), e76979, doi:10.1371/journal.pone.0076979, (2013).

12 Schnabel, L. V., Pezzanite, L. M., Antczak, D. F., Felippe, M. J. B. & Fortier, L. A. Equine bone marrow-derived mesenchymal stromal cells are heterogeneous in MHC class II expression and capable of inciting an immune response in vitro. *Stem Cell Research & Therapy.* **5** (1), 13-13, doi:10.1186/scrt402, (2014).

13 Taguchi, T. *et al.* Influence of hypoxia on the stemness of umbilical cord matrix-derived mesenchymal stem cells cultured on chitosan films. *Journal of Biomedical Materials Research Part B: Applied Biomaterials.* n/a-n/a, doi:10.1002/jbm.b.33864, (2017).

Supplemental File (Figures, Permissions, etc.)

Click here to download Supplemental File (Figures, Permissions, etc.)
Supplementary figure 1.tif